Article:
Penfold, N.J.W., Yeow, J., Boyer, C. et al. (2019) Emerging trends in polymerization-induced self-assembly. ACS Macro Letters, 8 (8). pp. 1029-1054. ISSN: 2161-1653

https://doi.org/10.1021/acsmacrolett.9b00464

Emerging Trends in Polymerization-Induced Self-Assembly

Nicholas J. W. Penfold,[a,†] Jonathan Yeow,[b,†] Cyrille Boyer,[b,*] and Steven P. Armes[a,*]

[a]*Department of Chemistry, The University of Sheffield, Brook Hill, Sheffield, South Yorkshire, S3 7HF, UK.*

[b]*Centre for Advanced Macromolecular Design (CAMD), School of Chemical Engineering, and Australian Centre for NanoMedicine, School of Chemical Engineering, UNSW Sydney, NSW 2051, Australia.*

Abstract: In this perspective, we summarize recent progress in polymerization-induced self-assembly (PISA) for the rational synthesis of block copolymer nanoparticles with various morphologies. Much of the PISA literature has been based on thermally-initiated reversible addition-fragmentation chain transfer (RAFT) polymerization. Herein, we pay particular attention to alternative PISA protocols, which allow the preparation of nanoparticles with improved control over copolymer morphology and functionality. For example, initiation based on visible light, redox chemistry, or enzymes enables incorporation of sensitive monomers and fragile biomolecules into block copolymer nanoparticles. Furthermore, PISA syntheses and post-functionalization of the resulting nanoparticles (e.g. crosslinking) can be conducted sequentially without intermediate purification by using various external stimuli. Finally, PISA formulations have been optimized via high-throughput polymerization and recently evaluated within flow reactors for facile scale-up syntheses.

1. Introduction

1.1 What is polymerization-induced self-assembly?

Block copolymer self-assembly is well-known in both the solid state[1-3] and also in solution.[4] In the latter case, a wide range of nano-objects have been prepared, including spheres, worms, rods, vesicles, lamellae, ellipsoids and toroids.[5-11] However, such nano-objects have been traditionally prepared via post-polymerization processing, which is typically conducted in dilute solution.[12-17] This is a significant limitation for many potential commercial applications, because it means that industrial scale-up is not normally cost-effective. Polymerization-induced self-assembly (PISA) offers an attractive solution to this problem. In a PISA formulation, a soluble precursor block is chain-extended using a monomer whose corresponding homopolymer is insoluble in the chosen solvent.[18-26] Thus, the growing second block eventually becomes insoluble at some critical degree of polymerization (DP), which drives *in situ* self-assembly to form the diblock copolymer nano-object. In this scenario, the unreacted monomer essentially acts as a processing aid or co-solvent for the insoluble block. PISA can be performed at relatively high solids (copolymer concentrations of up to 50% w/w)[27-28] and usually enables very high monomer conversions to be achieved within short reaction times compared to conventional solution polymerization.[29-30] This is because, once micellar nucleation occurs the unreacted monomer is preferentially located within the growing nanoparticles. This high local concentration leads to significant rate acceleration. Over the past decade or so, PISA has been demonstrated for a wide range of vinyl monomers in many solvents, including water,[18, 29, 31-35] polar solvents (e.g. ethanol),[36-41] non-polar solvents (e.g. *n*-alkanes)[28, 42-46] and other media such as ionic liquids,[47] silicone fluids[48] and supercritical CO_2.[49-53] If appropriate phase diagrams[54] are constructed, then PISA formulations become highly reproducible and the basic design rules for the preparation of spheres,[42, 55] worms,[32, 36, 46, 56] rods,[57] vesicles,[58-60] *framboidal* vesicles[59, 61-62] and lamellae[63-65] are now well-established in many cases. PISA syntheses have been conducted using various types of living polymerization techniques,[66-71] but many studies utilize reversible addition-fragmentation chain transfer (RAFT) polymerization due to its tolerance to a broad range of reaction conditions and monomer families.[72-77] The aim of this review is therefore to provide an insight into the broadening horizons of the PISA field with a particular focus on: **(1)** mechanisms for initiating and controlling the PISA process, **(2)** new insights

into stimuli responsive nanoparticle assemblies obtained via these new PISA processes, **(3)** emerging techniques for post-polymerization processing of PISA-derived nanoparticles, **(4)** the synthesis of advanced hybrid materials and **(5)** new strategies for improving the throughput and scale of the PISA process.

2. New Methods for Initiation during PISA

2.1 New stimuli for controlling PISA

The majority of PISA syntheses reported in the literature involve thermally-initiated controlled/living polymerizations. However in the last few years, there has been a surge of interest in new initiation mechanisms that utilize visible light,[78-83] microwaves,[84-87] enzymes,[88-92] electrochemistry,[93-97] or ultrasound.[98-101] Such alternative approaches open up new avenues of research for PISA formulations (**Figure 1**).

2.1.1 Photochemistry

The application of photochemistry to the field of polymer chemistry has been extensively explored in the past few years, not least because it can confer a high degree of spatiotemporal control. Furthermore, photopolymerizations can be conducted under mild reaction conditions (typically at ambient temperature or below) and can be performed using relatively inexpensive commercial light emitting diode (LED) sources or even natural sunlight.[102] Various visible light-mediated reversible deactivation radical polymerization (RDRP) (also referred to as controlled/living radical polymerization (CLRP)) formulations have been recently explored for the production of protein-polymer conjugates and functional polymer nanoparticles via photo-PISA approach.[103-104] The concept of photo-PISA was first demonstrated by Cai's group by employing a photoinitiator to initiate RAFT dispersion polymerization of diacetone acrylamide (DAAM) in water for the synthesis of amine-functional spheres.[33] Boyer's group expanded this concept by exploiting photoinduced electron transfer-reversible addition-fragmentation chain transfer (PET-RAFT) polymerization to synthesize nanoparticles with various morphologies (such as worms and vesicles) at ambient temperature.[105] The ability to target the worm phase was aided by *in situ* gelation of the reaction solution which occurs readily when PISA is performed at sufficiently high copolymer concentration. Through

judicious selection of the macro-RAFT agent, these polymerizations can also be initiated using visible light without requiring an external initiator or catalyst, thus simplifying this RAFT dispersion polymerization formulation.[106] Sumerlin, Zhang and co-workers employed a photoinitiator to initiate the polymerization of 2-hydroxypropyl methacrylate (HPMA) in water at 25 °C.[107] When targeting vesicle morphology, bovine serum albumin (BSA) was encapsulated within such hollow nanoparticles during their formation. Moreover, such mild reaction conditions ensured no denaturation of this globular protein, demonstrating that photopolymerization may offer useful advantages over thermally-initiated PISA.[107] Visible light initiated PISA has also opened up new possibilities for the synthesis of polymer-protein complexes and will be discussed further in **Section 5**. In a series of papers, Perez-Mercader and co-workers have employed visible light-mediated PISA to study the dynamic evolution of giant vesicles by monitoring their behavior during irradiation using a fluorescence microscope.[108-110] The mild conditions required for such PISA syntheses makes these experiments particularly convenient to perform.

2.1.2 Redox chemistry

Apart from photoinitiation techniques, alternative strategies for initiation during PISA have also emerged. Like photochemical initiation, radical generation via redox chemistry can be conducted under mild reaction conditions. However, the absence of an external stimulus eliminates the possibility of spatiotemporal control. For example, An's group employed a persulfate/ascorbate redox initiator system to prepare core-crosslinked nanogels at 30 ºC.[111] Later, the same group extended this concept by employing an enzyme, horseradish peroxidase (HRP), to catalyze the oxidation of acetylacetone by hydrogen peroxide and initiate the dispersion polymerization of 2-methoxyethyl acrylate (MEA) using biologically-relevant reaction conditions.[90] This PISA approach has also been coupled to an enzyme cascade reaction, whereby the hydrogen peroxide required for HRP-initiated polymerization was generated via glucose oxidase (GOx)-catalyzed reduction of molecular oxygen.[112] Very recently, the same group also utilized the flavin active site within GOx to conduct photoenzymatic initiation of RAFT dispersion polymerization.[113] These GOx based initiation methods allow PISA to be performed without prior deoxygenation of the reaction medium; such oxygen-tolerant PISA formulations will be discussed further in **Section 6**.

2.1.3 Ultrasound/Sonochemistry

Recently, several research teams have conducted RDRP using ultrasound by employing piezoelectric nanoparticles for mechno-atom transfer radical polymerization (ATRP)[98-100, 114] or by directly generating hydroxyl radicals in aqueous solution for either ICAR ATRP[115] or RAFT polymerization.[101, 116-117] Using the latter approach, Qiao's group employed high frequency ultrasound to initiate the aqueous dispersion polymerization of *N*-isopropylacrylamide (NIPAM) at 45 ^{o}C yielding thermosensitive core-crosslinked nanogels.[118] Using ultrasound as a stimulus can be considered to be environmentally-friendly because the initiating radicals are generated directly from the homolysis of water (which also acts as a solvent), hence no exogenous catalyst or initiator is required. The potential of this technique is yet to be fully explored in the context of PISA but may be limited by the need for specific ultrasound equipment.

2.1.4 Radiochemistry

Recently, Gianneschi, Sumerlin and coworkers demonstrated that under certain conditions the electron beam from a transmission electron microscope (TEM) could also be used to initiate RAFT polymerization by an iniferter type mechanism.[119] Elegantly, this process enabled an electron beam (with an electron flux of ~0.5 e^{-}/Å^2 s) to be used to both initiate and image the polymerization of HPMA in real time using a specialized liquid cell TEM. Although the full potential of such a technique is yet to be fully exploited, such strategies could be highly useful for improving our understanding of the morphological evolution that occurs during the PISA process.

2.2 Emerging polymerization mechanisms in PISA

The vast majority of PISA publications utilize RAFT polymerization to provide living/controlled character.[19, 72-77] Here, we wish to highlight exemplary examples whereby other living (and non-living) polymerization techniques have been applied to PISA. In the field of RDRP, Kim et al. demonstrated in 2005 the use of ATRP for the synthesis of core crosslinked nanogels via aqueous dispersion copolymerization of NIPAM with a bifunctional cross-linker at 50 °C.[120] Later, Matyjaszewski and co-workers demonstrated that ICAR ATRP could be used to synthesize a range of nano-objects in ethanol

similar to those achieved using RAFT-mediated PISA.[67] However, there are very few other examples for which ATRP-mediated dispersion polymerization has been used to prepare higher order morphologies.[68, 121] This most likely reflects the difficulty in controlling the location of the transition metal catalyst during dispersion/emulsion polymerization. Similarly, aside from pioneering work by Charleux and co-workers, there have been very few reports of non-spherical morphologies being obtained by nitroxide-mediated polymerization (NMP) using either dispersion or emulsion polymerization.[122-125] Recently, the groups of Goto[126] and Zhu[127] reported the use of iodine-mediated polymerization (ITP) for alcoholic PISA, generating nanoparticles without the use of either organosulfur compounds or transition metal catalysts.

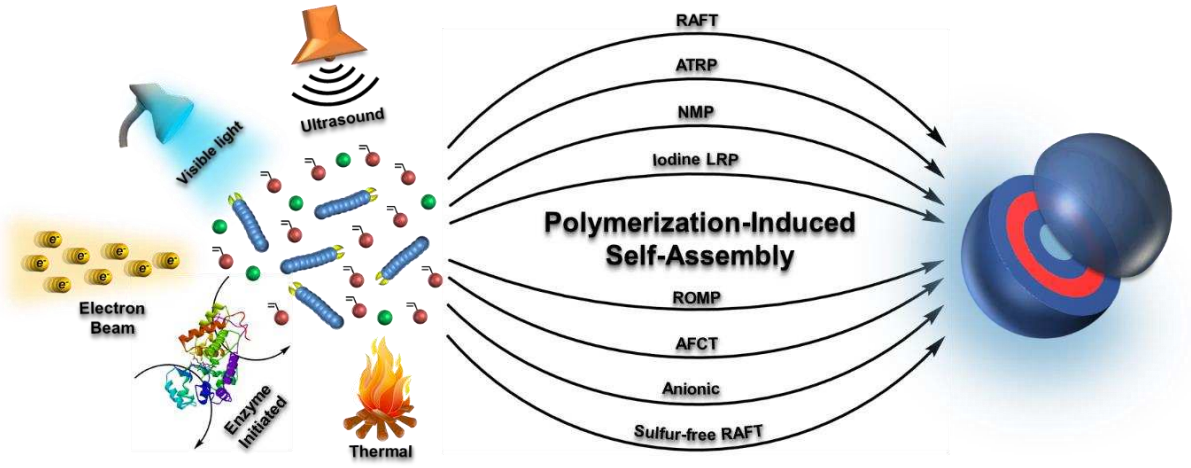

Figure 1. Summary of new approaches to PISA that utilize alternative initiation methods combined with various RDRP techniques.

Such strategies enable nanoparticles to be prepared without the need to remove colored thiocarbonylthio end-groups or potentially toxic metal residues (e.g. copper complexes). In addition, Zetterlund and co-workers examined a non-living form of radical polymerization known as addition-fragmentation chain transfer (AFCT) to prepare a range of nanoparticle morphologies in ethanol under PISA conditions without requiring a sulfur-based chain transfer agent.[128] Similarly, Bon and co-workers applied sulfur-free RAFT polymerization to develop an aqueous PISA formulation. However, both pre-assembly of the soluble precursor chains and a continuous monomer feed was required, while only relatively poor control and incomplete conversions were achieved.[129] Nonetheless, such approaches clearly warrant further studies, particularly for applications where colored copolymers, malodor or toxic residues would be problematic.

There has also been renewed interest in the use of living ionic polymerization techniques in PISA. For example, Manners' group built on the approach of Hasimoto and co-workers[130] by employing anionic polymerization for the PISA synthesis of highly anisotropic rods and platelets driven by crystallization of a structure-directing poly(ferrocenylmethylphenylsilane) block.[131] This approach enables crystallization-driven self-assembly (CDSA) to be performed at much higher concentrations than previously achieved. Others have explored the potential of ring-opening metathesis polymerization (ROMP) in PISA formulations by extending the seminal work of Xie and co-workers.[132] For example, Gianneschi's group performed ROMP dispersion polymerization of a peptide-functional norbornene monomer in methanolic DMF using a third-generation Grubbs catalyst.[133] More recently, O'Reilly's group developed an effective route for conducting aqueous ROMP PISA by first synthesizing a water-soluble macroinitiator in an organic solvent.[134] This strategy circumvents some of the limitations of conventional aqueous ROMP, enabling the *in situ* synthesis of a range of nanoparticle morphologies. Although the full potential of these techniques remains unfulfilled, these new strategies undoubtedly provide new impetus to the evolving PISA landscape.

2.3 New mechanisms of self-assembly within PISA

To date, self-assembly in the context of PISA has been almost exclusively driven by insolubility of the growing polymer block in the polymerization solvent. However, electrostatic interactions can also be utilized to drive self-assembly. For example, Cai and co-workers have combined electrostatic self-assembly with PISA to produce polymerization-induced electrostatic self-assembly (PIESA).[135] This can involve various approaches, such as polymerization of an ionic monomer in the presence of an oppositely-charged polyelectrolyte.[136-137] Recently, this concept was also extended to demonstrate the effect of comonomer distribution on the final nanoparticle morphology.[138] For example, the shape and size of vesicles/lamellae with identical chemical compositions could be tuned by varying the ionic comonomer distribution from block-like to a gradient-type distribution. In principle, PIESA is compatible with a broad range of ionic comonomers and it is clearly well-suited to aqueous formulations. Finally, block copolymer self-assembly can also be induced using the chemical ligation routes developed by Magenau's group[139] and Yan's group.[140] These strategies can be considered as alternatives to conventional PISA. However, given that self-

assembly is not induced by polymerization we consider these studies to be beyond the scope of this PISA-focused review.

3. Stimulus-responsive Block Copolymer Nano-objects

The number of examples of *stimulus-responsive* block copolymer nanoparticles prepared *via* PISA has grown considerably since the first example was published in 2012.[31] Much of this literature has focused on block copolymer nanoparticles that can change their morphology when exposed to a change in temperature,[31, 43, 56] pH,[141-144] light[145-146] or redox potential.[147] In many cases, the worm phase has been targeted. This is because this phase is relatively narrow, so such anisotropic nanoparticles can be often converted into spheres by applying a suitable stimulus. This morphological transition results in thermoreversible gelation, which may offer practical applications. Pei *et al.*[22] reviewed the field of stimulus-responsive nanoparticles in 2017. Thus, in the present article we briefly summarize the older literature and then focus on the most important advances made over the past two years.

3.1 Thermoresponsive Nanoparticles

In many cases, PISA formulations based on dispersion polymerization produce thermoresponsive diblock copolymer nano-objects. For example, in the case of aqueous dispersion polymerization, the second monomer (e.g. HPMA) is fully miscible in the aqueous continuous phase, which means that the insoluble block is usually only weakly hydrophobic. In contrast, aqueous emulsion polymerization involves *water-immiscible* monomers such as styrene or benzyl methacrylate, which leads to much more hydrophobic structure-directing blocks. In such cases, it is much less likely that thermoresponsive behavior will be observed for the resulting aqueous dispersions.[22] Indeed, there are numerous literature reports of kinetically-trapped spheres being obtained for the latter aqueous PISA formulations,[19, 27, 148] even when targeting highly asymmetric diblock copolymer chains that might be expected to form either worms or vesicles. This can be viewed as either a limitation or a benefit, as this morphological constraint actually provides a convenient low-viscosity route for the synthesis of high molecular weight hydrophobic polymer chains in aqueous media. In this context, Cockram *et al.* have recently postulated that the aqueous solubility of the second

monomer is likely to be a critical parameter for avoiding kinetically-trapped spheres, which is a common limitation for PISA syntheses based on aqueous emulsion polymerization formulations.[149]

Blanazs *et al.*[31] reported the first example of thermoresponsive block copolymer nano-objects prepared via PISA in 2012. More specifically, $PGMA_{54}$-$PHPMA_{140}$ (where PGMA = poly(glycerol monomethacrylate)) worms were prepared via RAFT aqueous dispersion polymerization of HPMA at 70 °C. This dispersion formed a soft physical gel on cooling to 20 °C. However, further cooling to 4 °C induced a worm-to-sphere transition, which led to concomitant degelation, as determined by variable temperature dynamic light scattering (DLS), TEM and small angle x-ray scattering (SAXS) studies. Moreover, ^{1}H NMR studies indicated greater solvation of the weakly hydrophobic PHPMA blocks at 4 °C, thus providing evidence for 'LCST-like' behavior.[150] Many non-ionic water-soluble polymers such as PNIPAM exhibit so-called 'inverse temperature solubility' behavior: they are soluble in cold water but become insoluble in hot water when heated above their lower critical solution temperature (LCST). The weakly hydrophobic PHPMA block exhibits similar temperature dependence for its degree of (partial) solvation but, unlike PNIPAM, it remains *water-insoluble* at all temperatures. These spectroscopic observations are interpreted in terms of greater solvation of the hydrophobic PHPMA block *close to the block junction* (see **Figure 2**).

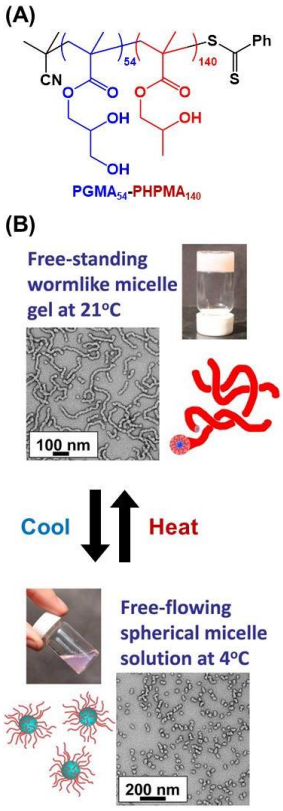

Figure 2. (A) Chemical structure of a $PGMA_{54}$-$PHPMA_{140}$ diblock copolymer. **(B)** Digital photographs, schematic cartoon and TEM images illustrating the thermoreversible behavior of this diblock copolymer. Cooling from 21 °C to 4 °C drives a worm-to-sphere transition and an associated gel-sol transition. Digital photographs were recorded at 10% w/w copolymer concentration. Adapted with permission from reference [31]. Copyright 2012 American Chemical Society.

Thus, it is believed that *surface plasticization* of the worms drives the worm-to-sphere transition. Temperature-dependent oscillatory rheology studies indicated that: (i) returning to 20 °C led to reformation of the original worms, albeit with some hysteresis and (ii) the reconstituted gel had essentially the same properties as the original worm gel. Moreover, these worm gels could be readily sterilized by ultrafiltration of the low-viscosity, free-flowing dispersion of spheres formed at 4 °C, which suggests potential biomedical applications. Indeed, Armes and co-workers demonstrated that similar $PGMA_{55}$-$PHPMA_{135}$ worm gels induce stasis (a quiescent, non-proliferative state) in pluripotent human stem cells[151] and can also be utilized for cryopreservation of red blood cells.[152] More recently, Lovett et al. reported that the gelation behavior of highly anisotropic diblock copolymer worms can be reasonably well explained in terms of percolation theory. This suggests that physical gelation is simply the result of multiple inter-worm contacts,[153] rather

than the 'worm entanglements' mechanism that has been invoked for surfactant-based worms.[154-155] Similarly, there are numerous literature reports of the preparation of thermoresponsive block copolymer nano-objects via *non-aqueous* dispersion polymerization. Thus, Fielding *et al.*[43] reported that poly(lauryl methacrylate)-poly(benzyl methacrylate) [PLMA-PBzMA] worms prepared in *n*-dodecane undergo a worm-to-sphere transition on heating to 90 °C. This change in morphology was confirmed by SAXS, TEM and DLS, with ^{1}H NMR spectroscopy studies indicating greater solvation of the core-forming PBzMA block at elevated temperature. Such thermoresponsive behavior is complementary to that observed in aqueous solution and thus can be interpreted in terms of 'UCST-like' behavior. In addition, Fielding *et al.* suggested that the worm-to-sphere transition was more likely to proceed by a 'worm budding' mechanism than by a 'random worm scission' mechanism.[43]

Subsequently, Lowe and co-workers reported that similar worm-to-sphere transitions could be obtained for several other methacrylic diblock copolymers in either alcohol[38, 156] or *n*-alkanes.[45, 157] These latter studies suggest that the structure-directing block should have a relatively low glass transition temperature, with chain mobility aiding the morphology transition. More recently, Warren *et al.*[158] compared the thermoresponsive behavior of three PGMA-PHPMA worms with differing block compositions: $PGMA_{37}$-$PHPMA_{80}$, $PGMA_{54}$-$PHPMA_{140}$ and $PGMA_{71}$-$PHPMA_{200}$ (see **Figure 3**).

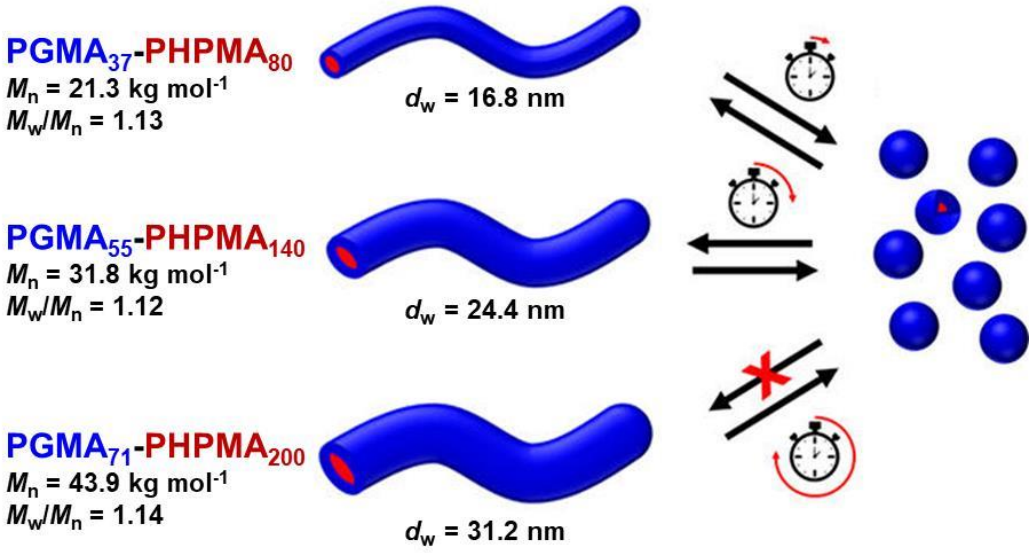

Figure 3. Schematic representation of three $PGMA_x$-$PHPMA_y$ diblock copolymer worms with differing mean cross-sectional worm diameters (d_w). The worm-to-sphere transition that is observed on cooling to 2

°C in each case is *reversible* for $PGMA_{37}$-$PHPMA_{80}$ and $PGMA_{55}$-$PHPMA_{140}$ but *irreversible* for $PGMA_{71}$-$PHPMA_{200}$. Adapted with permission from reference [158]. Copyright 2018 American Chemical Society.

Mean worm cross-sectional diameters were 16.9, 24.4 and 31.2 nm, respectively. In each case, concentrated aqueous dispersions of these worms formed free-standing gels at room temperature. Variable temperature SAXS studies were conducted to examine the effect of block composition on the thermoreversibility of the worm-to-sphere transition. On cooling to 2 °C, the $PGMA_{37}$-$PHPMA_{80}$ worms dissociated to form molecularly-dissolved copolymer chains. Returning to ambient temperature led to reformation of the worms, with recovery of the original gel strength. For the intermediate $PGMA_{54}$-$PHPMA_{140}$ composition, the worms formed sterically-stabilized spheres on cooling, rather than undergoing molecular dissolution. SAXS studies indicated that worms were reformed *via* stochastic 1D fusion of multiple spheres, even at copolymer concentrations as low as 0.5% w/w (given sufficiently long times). In contrast, $PGMA_{71}$-$PHPMA_{200}$ worms exhibited an *irreversible* worm-to-sphere transition. In summary, this study suggests that longer PHPMA chains become significantly more hydrophobic and ultimately no longer thermoresponsive. In retrospect, it is clear that the original observation of thermoreversible behavior for this particular PISA formulation was somewhat fortuitous. There are numerous literature examples for which a worm-to-sphere transition is *irreversible*.[59, 159-160] For example, Tan *et al.* prepared $PPEGMA_{14}$-$PHPMA_{200}$ (where PPEGMA = poly(poly(ethylene glycol) methyl ether methacrylate)) worms by photo-initiated PISA.[159] Cooling to 4 °C resulted in the desired worm-to-sphere and gel-sol transition. However, worm reformation did not occur on returning to room temperature, even after heating at 50 °C for 24 h. Similarly, Warren *et al.* reported that PEG_{113}-$PHPMA_{220}$ (where PEG = poly(ethylene glycol)) worms exhibited an irreversible worm-to-sphere transition on cooling.[59] In both cases, the observation of kinetically-trapped spheres suggests that steric stabilization is so efficient that it prevents the sphere-to-worm transition. HPMA monomer acts as a co-solvent/plasticizer for the growing insoluble PHPMA block during the initial PISA synthesis, which facilitates this evolution in morphology. This enhances the mobility of these growing chains, which aids 1D sphere-sphere fusion. However, once the polymerization is complete there is no longer any HPMA monomer to aid the sphere-to-worm transition. The thermoresponsive nature of PEG_{113} stabilized vesicles was also examined. The relatively large, polydisperse PEG_{113}-$PHPMA_{300}$ vesicles (D_h = 450 nm, PDI = 0.30)

originally obtained via PISA were transformed into spheres (D_h = 40 nm, PDI = 0.10) on cooling to 2 °C for 1 h. Incubation at 50 °C for 24 h led to the formation of much smaller, less polydisperse vesicles (D_h = 120 nm, PDI = 0.09). Utilizing this reversible thermal transition, a water-soluble rhodamine 6G-labeled poly((2-methacryloyloxy)ethyl phosphoryl-choline) (PMPC) homopolymer could be encapsulated within the lumen of the reformed PEG_{113}-$PHPMA_{300}$ vesicles. Thus, this protocol demonstrated the post-polymerization encapsulation of macromolecules within vesicles, with the significant reduction in vesicle dimensions also being preferred for potential intracellular delivery applications. However, one important question remains unclear: why do PEG_{113}-$PHPMA_{300}$ vesicles undergo a *reversible* morphology transition, whereas the PEG_{113}-$PHPMA_{220}$ worms exhibit an *irreversible* morphology transition?

The challenge of designing PEG-based diblock copolymer worms that undergo a *thermoreversible* worm-to-sphere transition was recently addressed by Penfold *et al*.[56] Assuming that the PEG_{113} stabilizer block is too long to allow the efficient 1D fusion of multiple spheres required to form worms, then reducing the mean DP of the PEG stabilizer block should enable a thermoreversible worm-to-sphere transition to be achieved. Utilizing a binary mixture of PEG_{113} and PEG_{45} macromolecular chain-transfer agents (macro-CTAs), a range of [x PEG_{45} + z PEG_{113}] – $PHPMA_n$ diblock copolymer nanoparticles were prepared. Here, x and z represent the mole fractions of the PEG_{45} and PEG_{113} stabilize blocks, respectively. A phase diagram was constructed to establish the relationship between block composition and copolymer morphology. The thermoresponsive behavior of each worm dispersion was evaluated by cooling a 10% w/w aqueous dispersion to 4 °C to induce a worm-to-sphere transition with concomitant degelation, followed by returning to 25 °C for 24 h. Almost all block copolymer compositions displayed *irreversible* behavior and are denoted by red filled squares in **Figure 4**.

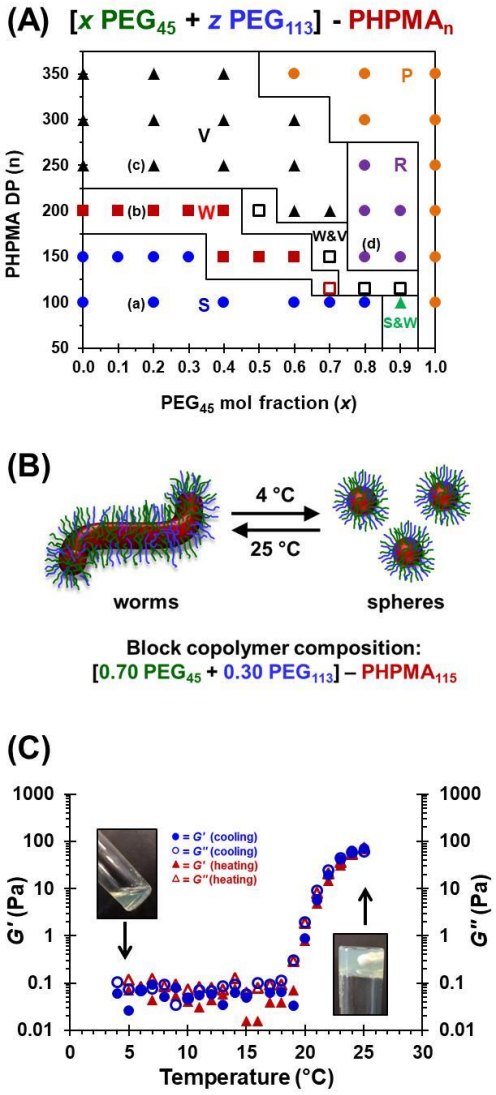

Figure 4. (A) Phase diagram constructed for [*x* PEG_{45} + *z* PEG_{113}] – $PHPMA_n$ to examine the relationship between block composition and copolymer morphology. Here *x* and *z* represent the mol fractions of PEG_{45} and PEG_{113} respectively and n represents the PHPMA DP [S = spheres, W = worms, V = vesicles, R = rosettes and P = precipitate]. (B) Schematic representation for the thermoreversible behavior exhibited by [0.70 PEG_{45} + 0.30 PEG_{113}] – $PHPMA_{115}$ worms. (C) Temperature-dependent oscillatory rheology data and digital photographs obtained for a 10% w/w aqueous dispersion of [0.70 PEG_{45} + 0.30 PEG_{113}] – $PHPMA_{115}$ worms subjected to a 25 °C – 4 °C – 25 °C thermal cycle. Adapted with permission from reference [56]. Copyright 2019 American Chemical Society.

However, a *single* composition corresponding to [0.70 PEG_{45} + 0.30 PEG_{113}] – $PHPMA_{115}$ worms exhibited thermoreversible behavior. Oscillatory rheology studies confirmed degelation at 4 °C, and the original gel strength was regained on returning to 25 °C. Furthermore, similar freeze-dried block copolymer worms

could be reconstituted after dissolution in a commercial cell culture medium (*Nutristem*) and the gel strength could be conveniently tuned by simply adjusting the copolymer concentration. Such thermoreversible worm gels should enable an important scientific question to be addressed: do human stem cells enter stasis when immersed within PGMA-PHPMA worm gels simply because of their very soft nature or is their hydroxyl-rich nature also important? Repeating such cell biology experiments using PEGylated worm gels of comparable softness should enable these two parameters to be delineated. In this context, it is also noteworthy that Ren and Perez-Mercader[161] prepared PEG_{45}-$PHPMA_x$ nano-objects using photo-initiated PISA at 25 °C. Colloidally stable dispersions were only obtained for PHPMA DPs of 60 to 80. PEG_{45}-$PHPMA_{80}$ spheres formed free-flowing liquids at 15 °C and very strong hydrogels (G' ~ 20 kPa) at 37 °C. Although this sol-gel transition was reversible, it was suggested to be the result of micelle network formation, rather than a worm-to-sphere transition. Furthermore, the bulk modulus is much too high for the long-term storage of stem cells, although other biomedical applications may be feasible.[151] As stated above, HPMA is a relatively rare example of a vinyl monomer that is suitable for aqueous dispersion polymerization. Alternative water-miscible monomers include NIPAM,[85] MEA,[111] *N,N*-diethylacrylamide (DEAA),[35] di(ethylene glycol) methyl ether methacrylate (DEGMA)[34] and DAAM.[33]

Over the past few years, DAAM has been evaluated by various research groups in the context of aqueous PISA formulations.[63, 162-165] This is in part because its reactive pendent ketone group provides a convenient platform for post-polymerization modification. For example, Byard *et al.*[32] synthesized poly(*N,N*-dimethyl acrylamide)-poly(diacetone acrylamide) PDMAC-PDAAM nanoparticles *via* RAFT aqueous dispersion polymerization at 70 °C. By varying the respective DPs of the PDMAC and PDAAM blocks, well-defined diblock copolymer spheres, worms or vesicles could be obtained. As for most PISA formulations, the worm phase proved to be the most difficult to identify and indeed this had eluded previous workers.[166-167] Even with the aid of a phase diagram, only a single diblock composition ($PDMAC_{40}$-$PDAAM_{99}$) could be identified that self-assembled to form pure worms. Given that DAAM monomer is highly water-soluble, it is perhaps surprising that such worms were not thermoresponsive when cooled to below 5 °C. However, heating to 50 °C resulted in a morphology transition from worms to a mixed phase comprising worms and vesicles.[32]

More recently, Wang *et al.*[63] prepared $PDMAC_{30}$-$PDAAM_x$ nanoparticles *via* RAFT aqueous dispersion polymerization at 70 °C. A phase diagram was constructed for this relatively short $PDMAC_{30}$ macro-CTA, which resulted in the *in situ* formation of lamellae and vesicles and the identification of an unusually broad lamellae phase. Moreover, $PDMAC_{30}$-$PDAAM_{60\text{-}90}$ lamellae were transformed into a mixture of worms and spheres on cooling from 70 °C to 10 °C. Rheology studies confirmed the expected sol-gel transition with a critical gelation temperature (CGT) of 35 °C. Returning to 70 °C resulted in lamellae reformation. Surprisingly, ^{1}H NMR studies over this temperature range indicated no detectable solvation for the core-forming PDAAM block. As expected, this thermoresponsive behavior was suppressed when the diblock copolymer lamellae were cross-linked *in situ* via statistical copolymerization of DAAM with 2 mol% allyl acrylamide.

To date, there appear to be no reports of aqueous thermoresponsive nanoparticles composed of an *all-acrylic* block copolymer. Presumably, this is in part because the relatively low T_g values of such copolymers makes TEM studies (and hence morphology assignments) somewhat problematic. In principle, the increasing availability of cryo-TEM facilities within many research institutes should enable such PISA formulations to be studied in the near future. In this context, it is perhaps noteworthy that Ratcliffe and co-workers constructed a useful phase diagram for the PISA synthesis of all-acrylic diblock copolymer nano-objects in non-polar media based mainly on DLS data and visual observations. This phase diagram was subsequently corroborated based on a relatively limited set of cryo-TEM observations.[168]

In a traditional PISA synthesis, the R group of the RAFT macro-CTA is a soluble polymer that acts as the steric stabilizer. After chain extension of this macro-CTA under PISA conditions, the organosulfur-based RAFT end-groups are located within the solvophobic interior of the nanoparticles.

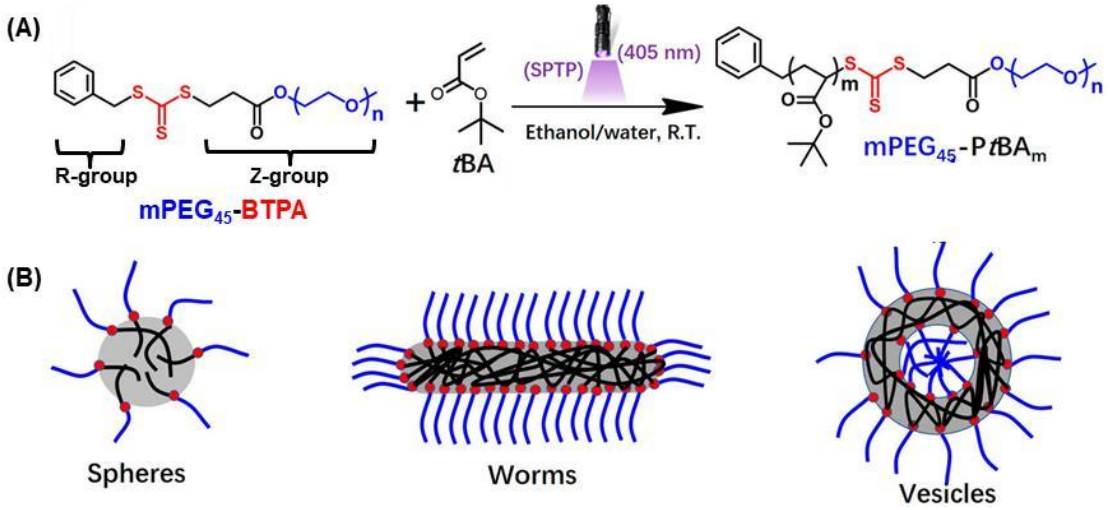

Figure 5. (A) Reaction scheme for the synthesis of mPEG$_{45}$-PtBA diblock copolymers *via* dispersion polymerization in ethanol/water mixtures. Note that a Z-type macro-CTA was utilized, where the PEG moiety is covalently attached to the Z-group of the RAFT agent. (B) Cartoon of mPEG$_{45}$-PtBA spheres, worms and vesicles. The red circles represent the location of the trithiocarbonate functionality of the RAFT agent at the core/shell interface. Adapted with permission from reference.[169] Copyright 2019 American Chemical Society.

In principle, an alternative approach would be to employ a macro-CTA[170-171] such that the steric stabilizer chain is effectively the Z group of the RAFT macro-CTA. In this case, the organosulfur component of the RAFT agent is located at the core-shell interface of the nanoparticles after PISA (**Figure 5B**). However, if the RAFT agent is not located within monomer-swollen nanoparticles, uncontrolled polymerizations are usually observed. In 2018, Tan *et al.*[169] reported the synthesis of a Z-type PEG$_{45}$ macro-CTA (see **Figure 5A**). 3-(Benzylthiocarbonothioylthio) propanoic acid (BTPA) RAFT agent was reacted with monohydroxy-capped PEG$_{45}$-OH to afford PEG$_{45}$-BTPA via Steglich esterification. This Z-type macro-CTA was then chain-extended with *t*-butyl acrylate in ethanol/water (60/40 w/w) mixtures at ambient temperature using photo-PISA. These conditions were selected to reduce monomer partitioning within the nanoparticles during PISA. This PISA synthesis involved RAFT dispersion polymerization using a sodium phenyl-2, 4, 6-trimethylbenzoylphosphinate (SPTP) photocatalyst. Canning *et al.*[172] reported that poly(*N,N*-dimethyl acrylamide)-poly(phenyl acrylate) [PDMAC-PPhA] nanoparticles could be synthesized by RAFT aqueous emulsion polymerization of phenyl acrylate. The unusually high T_g of 50 °C for the core-forming PPhA

block prevented film formation and allowed nanoparticle morphologies to be assigned by conventional TEM studies. As expected, only spherical nanoparticles were formed due to the low water-solubility of PhA monomer, a parameter believed to be critical in accessing more complex morphologies.[149]

In 2017, Pei *et al.*[22] reviewed the behavior of thermoresponsive nanoparticles in various organic solvents, with both worm-to-sphere and vesicle-to-sphere transitions being covered. Later that year, Derry *et al.*[173] demonstrated that $PSMA_{13}$-$PBzMA_{96}$ (where PSMA = poly(stearyl methacrylate)) vesicles prepared in mineral oil undergo a vesicle-to-worm transition on heating up to 150 °C. TEM images confirmed the formation of highly anisotropic worms, while SAXS analysis of the initial and final copolymer morphologies indicated that, on average, each vesicle dissociated to form approximately three worms. Variable temperature ^{1}H NMR studies indicated an apparent degree of solvation of up to 43% for the PBzMA core-forming block at 150 °C, and the morphology transition was explained in terms of surface plasticization of the vesicle membrane. Perhaps more importantly, this vesicle-to-worm transition leads to a significant increase in solution viscosity at elevated temperature. Thus, in principle, such a change in copolymer morphology offers a completely new high-temperature oil-thickening mechanism.

3.2 pH, Photo- and Redox-responsive Nanoparticles

In their 2017 review article, Pei *et al.* also discussed pH-responsive block copolymer nanoparticles prepared via PISA.[22] For example, Armes and co-workers reported that essentially *non-ionic* PGMA-PHPMA nano-objects can exhibit fully reversible worm-to-sphere transitions. Importantly, these diblock copolymers were prepared using either a carboxylic acid[144] or morpholine-functionalized[142] RAFT agent, with such groups being located at the terminus of the PGMA stabilizer chains. Ionization of the carboxylic acid group or protonation of the morpholine end-group resulted in a subtle increase in the volume fraction of the PGMA block, which in turn drives a worm-to-sphere transition. Furthermore, the analogous vesicle-to-worm transition was also reported for similar PISA formulations.[141, 143] Perhaps unsurprisingly, these morphology transitions were suppressed in the presence of added salt owing to charge-screening effects. In closely related work, Gibson *et al.*[174] recently prepared a series of seven poly(*N*-(2-methacryloyloxy)ethyl pyrrolidone) [PNMEP] homopolymers with a range of DPs using a carboxylic acid-based RAFT agent.

Ionization of this end-group was shown to be essential for the formation of colloidally stable nanoparticles prepared via aqueous PISA. More specifically, the RAFT aqueous dispersion polymerization of HPMA and the RAFT aqueous emulsion polymerization of 2-ethoxyethyl methacrylate (EEMA) were both unsuccessful when conducted at pH 3 but yielded anionic electrosterically-stabilized nanoparticles when performed at pH 7. Both PNMEP-PHPMA and PNMEP-PEEMA spheres exhibited zeta potentials of approximately −30 mV at pH 7. However, protonation of the anionic carboxylate end-group resulted in irreversible flocculation at pH 3, which confirmed that such end-groups made a vital contribution to the overall colloidal stability. This was further confirmed by the addition of electrolyte, with flocculation being observed at a KCl concentration of 60 mM.

Poly(2-(diisopropylamino)ethyl methacrylate) [PDPA] exhibits pH-dependent aqueous solubility.[175] As a weak polybase with a pK_a of around 6.2, PDPA is insoluble in neutral or basic solution but dissolves in acidic solution owing to protonation of its tertiary amine groups. This pH-dependent solubility also applies to DPA monomer. In 2018, Mable *et al.*[61] chain-extended $PGMA_{58}$-$PHPMA_{300}$ vesicles using DPA *via* RAFT seeded emulsion polymerization. The precursor $PGMA_{58}$-$PHPMA_{300}$ vesicles exhibited smooth surfaces and remained intact between pH 3 and pH 8. However, the resulting $PGMA_{58}$-$PHPMA_{300}$-$PDPA_{86\text{-}460}$ vesicles had a distinctly *framboidal* morphology. This was explained in terms of microphase separation between the mutually incompatible hydrophobic PHPMA and PDPA blocks, which leads to the protrusion of nano-sized PDPA spherical globules from the vesicle membranes. Larger globules were observed when targeting higher PDPA DPs. Importantly, vesicle disintegration occurred on lowering the dispersion pH to pH 3. Below the pK_a of the PDPA block, the tertiary amine groups become protonated and acquire cationic character. This resulted in an irreversible loss of the *framboidal* vesicle morphology to produce ill-defined weakly-interacting spheres according to TEM analysis. SAXS studies indicated the presence of a fractal-like morphology at pH 3. Time-resolved pH-jump SAXS experiments confirmed that vesicle disintegration occurred rapidly and was complete within 1 s.

Like DPA, 2-(diethylamino)ethyl methacrylate (DEA) is a weak base (pK_a ~ 7.3) that exhibits pH-responsive behavior.[175] PDEA is hydrophobic in its neutral form but becomes hydrophilic when protonated (**Figure 6A**).

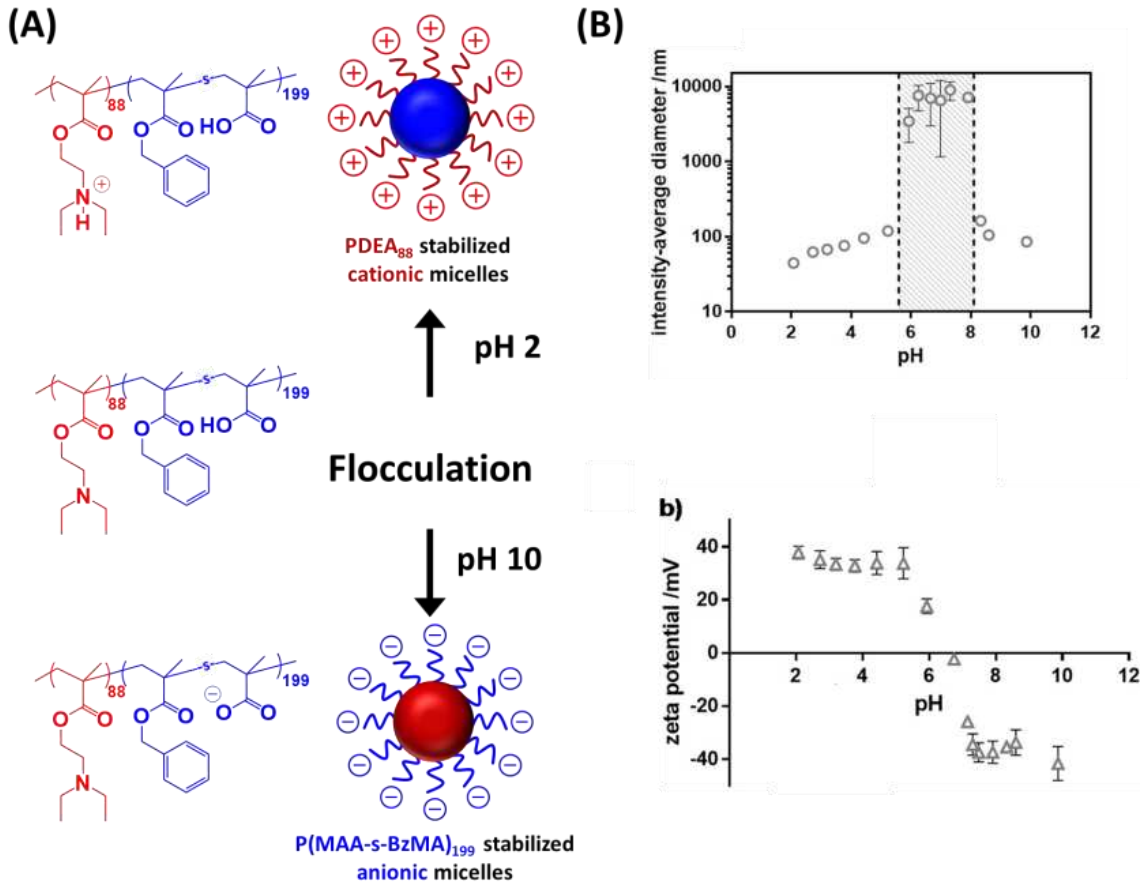

Figure 6. (A) Chemical structure and schematic representation of the schizophrenic behavior exhibited by $PDEA_{88}$-P(MAA-*stat*-BzMA)$_{199}$ diblock copolymer nanoparticles in aqueous solution on adjusting the solution pH. (B) Variation in intensity-average diameter and zeta potential with pH for a 0.1% w/w dispersion of $PDEA_{88}$-P(MAA-*stat*-BzMA)$_{199}$ diblock copolymer spheres. Adapted with permission from reference [176]. Copyright 2019 American Chemical Society.

Taking advantage of this pH-responsive character, Canning *et al.*[176] reported that pH-responsive $PDEA_{88}$-P(MAA-*stat*-BzMA)$_{199}$ (where MAA = methacrylic acid) diblock copolymer spheres can be prepared at pH 2.5 via RAFT aqueous emulsion copolymerization of MAA and BzMA. The P(MAA-*stat*-BzMA) block is a weak polyacid. Thus, PISA synthesis conducted under acidic conditions produces cationic diblock copolymer spheres of approximately 40 nm diameter, with electrosteric stabilization conferred by the protonated $PDEA_{88}$ stabilizer chains and the spherical cores being composed of the protonated hydrophobic P(MAA-*stat*-BzMA) block (**Figure 6B**). On addition of base, the PDEA residues become less protonated and macroscopic precipitation was observed at around the isoelectric point. A colloidal dispersion

comprising highly anionic nanoparticles was obtained above pH 8. ^{1}H NMR spectroscopy studies confirmed that the PDEA block now forms the insoluble micelle cores under such conditions, while the ionized P(MAA-*stat*-BzMA) chains are located within the micelle corona. This is an example of so-called 'schizophrenic' micellization behavior.[177]

A third commercially available tertiary amine methacrylate is 2-(dimethylamino)ethyl methacrylate (DMAEMA). This monomer has a similar pK_a to that of DEA but it is water-miscible even in its neutral form. Tan *et al.* prepared a poly(ethylene glycol) methyl ether methacrylate (PEGMA, M_n = 475 g mol^{-1}) macro-CTA with a mean DP of 9 and chain-extended PPEGMA$_9$ *via* RAFT aqueous dispersion copolymerization of HPMA with DMAEMA using photo-PISA at 25 °C to prepare PPEGMA$_9$-P(HPMA-*stat*-DMAEMA) vesicles.[178] Bubbling CO_2 into this aqueous dispersion lowered the pH owing to the formation of carbonic acid (H_2CO_3). In control experiments, PPEGMA$_9$-PHPMA$_{200}$ vesicles remained essentially unchanged in the presence of CO_2. However, when PPEGMA$_9$-P(HPMA$_{200}$-*stat*-DMAEMA$_{10}$) vesicles were exposed to CO_2, they were transformed into "irregular nanoparticles", with DLS studies indicating a reduction in mean nanoparticle diameter from 404 nm to 188 nm. The DMAEMA residues are protonated at low pH, so the membrane-forming block becomes less hydrophobic. This subtle change in solvation drives the observed morphology transition. Incorporating higher amounts of DMAEMA into the PPEGMA$_9$-P(HPMA$_{200}$-*stat*-DMAEMA$_{40}$) vesicles led to a vesicle-to-chain transition on exposure to CO_2: the original milky-white dispersion became transparent and nanoparticles could no longer be observed by DLS or TEM. Finally, a model protein (BSA) could be encapsulated within PPEGMA$_9$-P(HPMA$_{200}$-*stat*-DMAEMA$_{80}$) vesicles with a loading efficiency of 24%, with protein release occurring after CO_2 treatment. It is well-known that bubbling nitrogen gas through CO_2-saturated aqueous solution can remove the dissolved gas and return the solution pH to its original neutral value.[179] Thus it is perhaps surprising that Tan *et al.* did not examine the reversibility of this morphological transition.

Coumarin is a well-known light-sensitive compound that has been used to design light-responsive block copolymers.[180-184] Hydroxyl-functional derivatives of coumarin can be reacted with methacryloyl chloride to produce coumarin-based methacrylates, such as 7-(2-methacryloyloxyethoxy)-4-methylcoumarin (CMA).[183] Utilizing CMA, Pan and co-workers[185] recently reported that PHPMAC$_{40}$-P(DPA$_{80}$-*stat*-CMA$_{20}$) spheres,

'nanowires' or vesicles could be prepared in an 70/30 w/w ethanol/water mixture at 20% w/w solids. UV irradiation at 365 nm led to vesicle cross-linking via photo-triggered dimerization of the coumarin groups within the membrane-forming block. DLS studies indicated that the cross-linked vesicles had an intensity-average diameter of 440 nm at pH 8. However, the vesicles swelled to 820 nm at pH 4 owing to protonation of the DPA residues within the hydrophobic membrane. These vesicle dimensions remained constant for five pH cycles between pH 8 and pH 4. Moreover, the mean size of membrane pores could be fine-tuned by varying the UV irradiation time to adjust the cross-link density. Gold nanoparticles of up to 15 nm diameter could be 'post-loaded' within such porous vesicles.

More recently, the same team reported the PISA synthesis of dual-responsive vesicles.[186] PEG_{90}-$PDPA_X$ vesicles were prepared in the presence of a bifunctional cross-linker, cystamine bismethacrylamide (CBMA) (**Figure 7**). The lower reactivity of CBMA compared to DPA ensured that cross-linking was delayed until vesicles had been formed. These vesicles proved to be pH-responsive, with mean diameters ranging from 300 nm to 600 nm over three pH cycles. Moreover, addition of a reductant (DTT) cleaved the disulfide bonds within the CBMA residues, causing vesicle molecular dissolution within 20 min at pH 4. However, if the same DTT cleavage experiment was conducted at pH 8, then the vesicles remained intact because the DPA residues within the membrane-forming block are highly hydrophobic under such conditions.

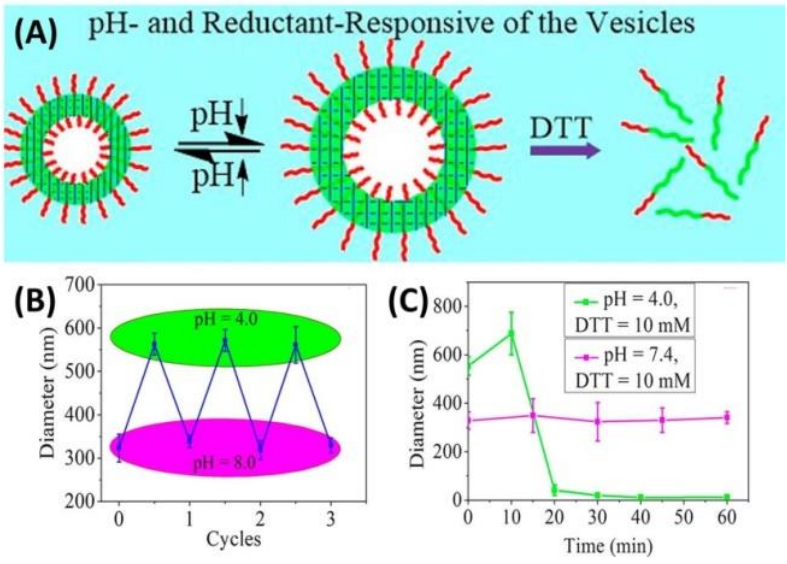

Figure 7. (A) Schematic representation of the pH-responsive swelling exhibited by PEG-P(DPA-*stat*-CBMA) vesicles. (B) pH cycling experiments confirm the reversibility of the change in vesicle dimensions.

(C) Addition of a suitable reductant (e.g. DTT) at pH 4 leads to cleavage of the disulfide bonds within the CBMA cross-links; such vesicles undergo molecular dissolution under these conditions because the DPA residues are protonated at this pH. Conversely, the same vesicles remain intact if the DTT reagent is added at pH 7.4. Adapted with permission from reference [186]. Copyright 2019 American Chemical Society.

Recently, Boyer and co-workers reported the synthesis of redox responsive poly(oligo(ethylene glycol) methyl ether methacrylate-poly(2-(methylthio)ethyl methacrylate) [POEGMA-PMTEMA] nanoparticles under ethanolic Photo-PISA conditions.[178] Interestingly, the thioether functional and water insoluble PMTEMA block could be readily oxidized to the corresponding polymeric sulfoxide yielding a double hydrophilic block copolymer. This mechanism was used to demonstrate the disassembly of POEGMA-PMTEMA vesicles in the presence of hydrogen peroxide. Alternatively, such POEGMA-PMTEMA vesicles were also shown to be responsive to visible light with nanoparticle disassembly occurring due to the generation of singlet oxygen by an encapsulated photosensitizer.

Sobotta *et al.*[147] employed an aqueous one-pot RAFT-mediated PISA protocol to prepare a series of novel redox-responsive poly(*N*-acryloylmorpholine)-poly(*N*-acryloylthiomorpholine) (PNAM-PNAT) nanoparticles (see **Figure 8**).

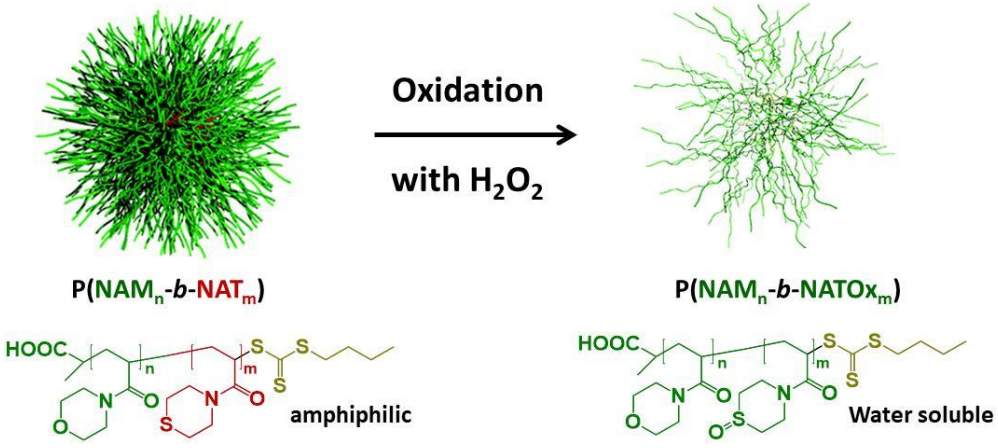

Figure 8. Schematic representation of the oxidation-induced degradation of PNAM-PNAT nanoparticles to water soluble chains after exposure to H_2O_2. Adapted with permission from reference [147]. Copyright 2017 Royal Society of Chemistry.

Like PMTEMA, PNAT is insoluble in water but oxidation of its thioether moiety yields a sulfoxide species and the resulting PNATOx block is water-soluble. Thus exposing PNAM-PNAT spherical nanoparticles to relatively low concentrations of hydrogen peroxide resulted in nanoparticle dissociation to form water-soluble diblock copolymer chains. Moreover, such redox-responsive nanoparticles were shown to be biocompatible. Thus, in principle, such redox responsive polymeric nanoparticles could provide a convenient mechanism for the delivery of hydrophobic drugs to specific sites that are subjected to localized oxidative stress.

4. New Strategies for Cross-linking

It is well-known that linear block copolymer nanoparticles undergo either dissociation to individual copolymer chains or a change in copolymer morphology when exposed to (i) surfactants, (ii) good solvents for both blocks, or (iii) changes in temperature or solution pH.[187] To address this problem, a wide range of chemistries have been utilized to prepare covalently-stabilized block copolymer nanoparticles,[188-189] including those prepared via PISA.[21, 190] Most examples focus on core cross-linking, because conducting shell cross-linking at high copolymer concentrations usually results in inter-particle cross-linking and hence irreversible loss of colloidal stability. Generally speaking, cross-linking can be performed either via post-polymerization derivatization or during the polymerization. These two strategies are discussed in turn below.

4.1 Post-polymerization cross-linking of nanoparticles.

In principle, covalently-stabilized block copolymer nanoparticles can be conveniently prepared via PISA simply by adding a divinyl comonomer such as ethylene glycol dimethacrylate (EGDMA). In principle, such comonomers can be added during the initial growth of the core-forming block.[191] However, better results are usually obtained when adding EGDMA to linear diblock copolymer nanoparticles to produce core-cross-linked ABC triblock copolymer nanoparticles, where the C block comprises PEGDMA (**see Scheme 1A**). Armes and co-workers have shown that this strategy can work well for both spheres[192] and vesicles[193] but it is more problematic for worms. This is because the latter morphology occupies relatively narrow phase space. Thus, targeting even a relatively short PEGDMA block can generate mixed phases. Nevertheless, core cross-linked worms can be prepared by this route if sufficient care is exercised.[192]

In some cases, post-polymerization cross-linking can be readily achieved with no change in the block copolymer composition. For example, PDMAC-PDAAM diblock copolymer nano-objects prepared via RAFT aqueous dispersion polymerization can be covalently stabilized using adipic dihydrazide (ADH) in concentrated aqueous solution (**see Scheme 1B**).[32, 162] However, it is perhaps more common to introduce comonomers with appropriate functionality into the PISA formulation. One of the most versatile comonomers in this regard is glycidyl methacrylate (GlyMA), because its pendent epoxy groups can be readily cross-linked via various chemistries. These include reaction with diamines (**see Scheme 1C**),[194-195] 3-aminopropylsiloxane (APTES) (see Scheme 1D)[196-198] or 3-mercaptopropylsiloxane (MPTES).[199]

For example, Chambon *et al.*[194] prepared $PGMA_{55}$-P($HPMA_{247}$-*stat*-$GlyMA_{82}$) diblock copolymer vesicles via RAFT aqueous dispersion copolymerization of HPMA and GlyMA. It is well-known that surfactants can disrupt vesicle membranes and cause rapid vesicle disintegration. To address this problem, various diamines such as ethylenediamine or commercially available Jeffamines were added to concentrated aqueous dispersions of the vesicles to enhance their stability. Ring-opening of the epoxy groups within the vesicle membranes by such diamines resulted in cross-linking, which dramatically increased vesicle stability in the presence of surfactants. This approach is attractive because the GlyMA monomer is commercially available, relatively cheap, and a range of bifunctional nucleophiles can be utilized to cross-link such nanoparticles.

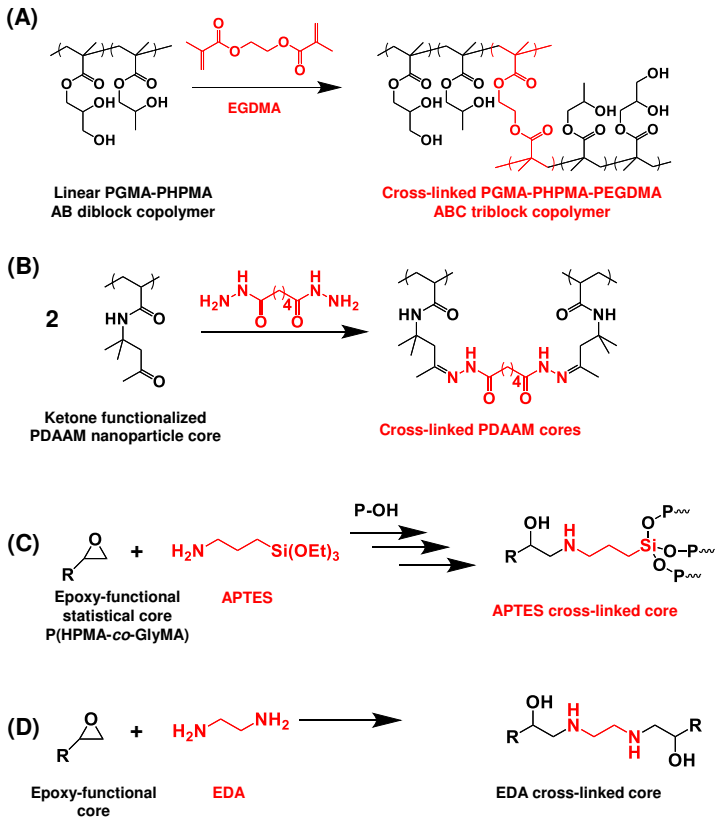

Scheme 1. Various strategies reported in the literature to covalently stabilize block copolymer nanoparticles prepared via RAFT-mediated PISA. (A) Polymerization of ethylene glycol dimethacrylate (EGDMA) as the 'C' block to produce ABC triblock copolymer vesicles with cross-linked membranes;[193] (B) Addition of adipic dihydrazide (ADH) to ketone-functional poly(diacetone acrylamide) (PDAAM) cores leads to hydrazone cross-links between chains;[32, 162] (C) Addition of 3-aminopropyltriethoxysilane (APTES) to epoxy-functional nanoparticles enables core cross-linking via simultaneous epoxy-amine chemistry and siloxane hydrolysis with concomitant condensation of the resulting silanol groups and the hydroxyl groups on neighbouring HPMA residues;[197] (D) ring-opening of the pendant epoxy groups in glycidyl methacrylate-based spherical nanoparticles with ethylenediamine.[200] [P-OH denotes the hydroxyl functionality located within P(HPMA-*co*-GlyMA) cores].

An alternative cross-linking strategy for diblock copolymer nano-objects was reported by Lovett *et al.*,[197] who prepared five examples of $PGMA_{56}$-P($HPMA_y$-*stat*-$GlyMA_z$) worms (where y, z were varied and y + z = 144).The GlyMA content could be varied from zero to 20 mol% without perturbing the copolymer morphology. Covalent cross-linking of the worm cores was achieved by addition of APTES. The pendent epoxy groups in the GlyMA residues reacted with the primary amine group on the APTES, with covalent

cross-linking resulting from simultaneous hydrolysis/condensation of the pendent siloxanes, both with each other and with the secondary hydroxyl groups on the HPMA residues. Kinetic studies using ^{1}H NMR spectroscopy revealed that the ring-opening and hydrolysis/condensation reactions occurred on similar time scales, suggesting that they proceeded concurrently, rather than sequentially. Successful cross-linking was assessed by dilution into methanol (a good solvent for both linear blocks) with subsequent TEM analysis confirming retention of the worm morphology. The cross-linked worms also proved to be colloidally stable in the presence of excess anionic surfactant (SDS). APTES cross-linking resulted in stiffer worms and the acquisition of weak cationic character owing to secondary amine formation within the worm cores. In principle, less APTES should be required compared to a diamine cross-linker, because the former reagent can theoretically react with up to four other copolymer chains.

Recently, Hunter *et al.*[196] utilized this APTES cross-linking chemistry to prepare two types of $PGMA_{48}$–P($HPMA_{90}$-*stat*-$GlyMA_{15}$) diblock copolymer worms that differed only in their mean aspect ratio. This was achieved by conducting the APTES cross-linking at two different temperatures to take advantage of the weakly thermoresponsive nature of the core-forming P($HPMA_{90}$-*stat*-$GlyMA_{15}$) chains.[191] Thus relatively long cross-linked worms were prepared by reaction with APTES at 20 °C for 24 h, whereas relatively short worms were obtained using the same reagent at 4 °C for 7 days. According to SAXS studies, these two types of worms had mean aspect ratios of approximately 40 and 5, respectively. Both types of worms were used as Pickering emulsifiers to prepare *n*-dodecane-in-water emulsions, which were then exposed to a non-ionic surfactant (Tween 80). Significantly higher surfactant concentrations were required to displace the longer worms from the oil/water interface. Thus this study demonstrated that highly anisotropic nanoparticles are more effective Pickering emulsifiers than less anisotropic nanoparticles with essentially the same chemical composition.

Covalent stabilization of highly anisotropic block copolymer worms also enables their use as highly effective flocculants for model micrometer-sized particles. Thus, Penfold *et al.*[198] utilized the same GlyMA/APTES strategy to prepare cationic cross-linked worms by employing a binary mixture comprising 90% PEG_{113} and 10% $PQDMA_{125}$ macro-CTAs. Unlike the linear worms, the cationic cross-linked worms (zeta potential ~ +40 mV) remained colloidally stable when challenged with methanol (a common solvent

for both blocks) or a cationic surfactant (CTAB). Both the linear and cross-linked cationic worms were evaluated as putative flocculants for near-monodisperse 1 μm diameter anionic silica particles. Once electrostatically adsorbed, the linear cationic worms did not survive the strong torsional forces exerted by the relatively massive anionic silica particles. Thus only minimal flocculation was observed by laser diffraction ($D_{4/3}$ ~ 3 μm). Conversely, the covalently cross-linked worms proved to be sufficiently robust to cause substantial silica flocculation ($D_{4/3}$ ~ 30 μm for the resulting aggregates). Scanning electron microscopy (SEM) studies confirmed that the electrostatically-adsorbed cross-linked worms acted as bridging flocculants by spanning between neighboring silica particles. Importantly, these cross-linked cationic worms outperformed four commercially-available high molecular weight water-soluble polymers that are widely used as flocculants. Moreover, such cross-linked cationic worms were also able to flocculate 4 μm and 8 μm silica spheres. In related work,[199] both cationic and anionic cross-linked worms were prepared using a binary mixture of a non-ionic and a polyelectrolytic steric stabilizer block. In this case, covalent stabilization was achieved by reacting MPTES with GlyMA residues within the worm cores rather than APTES. This is because the epoxy-thiol reaction produces neutral species and hence does not adversely affect the electrophoretic behavior of the original worms. Aqueous electrophoretic studies indicated zeta potentials of ~ +41 mV and -39 mV for the cationic and anionic worms, respectively. Layer-by-layer (L-b-L) deposition of these cationic and anionic cross-linked worms was performed in turn on planar silicon wafers. Such experiments were conducted to gain a better understanding of the well-known L-b-L deposition of soluble polyelectrolytes in the absence of salt because the much greater length scale of the worms was sufficient to enable their direct visualization by SEM. Interestingly, the deposition of cross-linked cationic worms onto a planar anionic silicon wafer (layer 1) was extremely fast, with ~16% surface coverage being obtained within a few seconds. Subsequent L-b-L deposition of oppositely-charged worms resulted in a gradual increase in surface coverage as judged by ImageJ analysis of SEM images. Surface zeta potential studies confirmed that this sequential deposition was accompanied by charge reversal for each new worm layer. Interestingly, ellipsometry studies revealed two linear growth regimes, with faster film growth obtained after approximately monolayer coverage.

GlyMA is a water-immiscible monomer with an aqueous solubility of ~ 24 g dm^{-3} at 80 °C.[201] Thus using solely GlyMA to generate a core-forming block via aqueous PISA should involve emulsion polymerization. According to the PISA literature formulations based on emulsion polymerization are often limited to kinetically-trapped spheres, although non-spherical morphologies have occasionally been reported.[149, 202-206] Recently, Hatton *et al.*[195] reported the synthesis of $PGMA_{45}$-$PGlyMA_x$ diblock copolymer nanoparticles at 50 °C by RAFT aqueous emulsion polymerization. Only spherical nanoparticles were obtained, although their mean diameter could be tuned by systematic variation of the PGlyMA DP. Core cross-linking of $PGMA_{45}$-$PGlyMA_{100}$ spheres was performed using either ethylenediamine or bis(3-aminopropyl)-terminated PEG (PEG_{31}-DA). This led to the formation of core cross-linked nanogels, which acquired weakly cationic character due to their secondary amine functionality. One way to access diblock copolymer worms and vesicles comprising solely PGlyMA cores is to switch from purely aqueous media to using ethanol/water mixtures. For example, Tan *et al.*[200] chain-extended a PEG_{45} macro-CTA with GlyMA using a 40:60 w/w ethanol/water mixture at 25 °C using photo-PISA. Importantly, this solvent composition is a good solvent for GlyMA monomer but the resulting PGlyMA is insoluble, allowing the formation of spheres, worms and vesicles via RAFT dispersion polymerization. ^{1}H NMR spectroscopy studies indicated up to 98% of the original epoxy groups survive under such mild reaction conditions. Cross-linked block copolymer worms and vesicles were then obtained by reacting with ethylenediamine at room temperature.

GlyMA has also been used as a core-forming monomer for PISA syntheses conducted in mineral oil. For example, Docherty *et al.*[207] chain-extended a PSMA macro-CTA with GlyMA to prepare PSMA-PGlyMA spheres of tunable diameter. According to ^{1}H NMR studies, essentially all of the epoxy groups survived the PISA synthesis, with enhanced long-term stability being observed compared to PGlyMA-core nanoparticles synthesized via RAFT aqueous emulsion polymerization of GlyMA.[195] The epoxy-functional spheres prepared in mineral oil were subsequently reacted with *N*-methylaniline. Ring-opening of the epoxy group by this secondary amine produced hydroxyl groups, which ultimately resulted in core cross-linking.

More recently, use of a ketone-functionalized monomer, DAAM as the core-forming block in PISA formulations has provided new opportunities to explore various cross-linking chemistries. Importantly, the full range of nanoparticle morphologies can be accessed via RAFT aqueous dispersion polymerization of

DAAM using either photo-PISA or thermally-initiated PISA.[32-33, 63, 162, 164, 166] For example, Byard *et al.*[32] reported cross-linking of PDMAC-PDAAM spheres, worms and vesicles by reacting the ketone moieties with ADH. Sufficient cross-linking for covalent stabilization was achieved within 6 h at 25 °C using [ADH]/[DAAM] molar ratios as low as 0.075. Such post-polymerization modification did not perturb the original worm morphology. Similarly, Figg *et al.*[162] cross-linked PDMAC-P(DMAC-*stat*-DAAM) diblock copolymer nano-objects using a difunctional alkoxyamine at 70 °C, resulting in hydrolytically stable oxime linkages. In this study, the composition of the core-forming block was systematically varied to control the mean length of the block copolymer worms.

DAAM has also been used as a *stabilizer* block in PISA formulations. He *et al.*[208] chain-extended a $PDAAM_{29}$ macro-CTA with *t*-butyl acrylate (*t*BA) via photo-PISA in a 60/40 w/w ethanol/water mixture. Spheres, worms and vesicles were prepared, but the worm phase space was extremely narrow when $PDAAM_{29}$-P*t*BA_{69} diblock copolymers were prepared at 30% w/w. Incorporation of isobornyl acrylate into the core resulted in the formation of lamellae, which could be subsequently shell cross-linked *via* the PDAAM stabilizer chains using ADH at 5% solids. Subsequent hydrolysis of the *t*BA residues produced carboxylic acid groups, which could be used as a template for the formation of silver nanoparticles via *in situ* reduction of $AgNO_3$. It is clear that low molecular weight polyfunctional reagents offer a convenient post-polymerization approach to produce covalently-stabilized block copolymer nanoparticles (see **Scheme 2**). However, specific functionality (usually epoxy or ketone groups) must be incorporated into the nanoparticles if this strategy is to be successfully implemented.

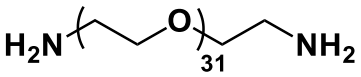

PEG$_{31}$-diamine

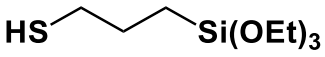

MPTES

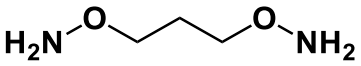

1,3-bis-aminooxypropane

Scheme 2. Chemical structures of three low molecular weight reagents that have been employed to covalently cross-link various types of block copolymer nanoparticles prepared via PISA; PEG$_{31}$-diamine,[195] 3-mercaptopropylsiloxane (MPTES)[199] and 1,3-bis-aminooxypropane.[162]

However, this approach is not the only strategy for the preparation of core cross-linked nanoparticles. For example, we have already discussed use of the photo-reactive CMA[183-184] as a core-forming block in PISA formulations to prepare cross-linked PHPMAC$_{40}$-P(DPA$_{80}$-*stat*-CMA$_{20}$) nanoparticles via UV irradiation (λ = 365 nm). Similarly, PHPMAC-P(NBMA-*stat*-CMA) (where NBMA = 2-nitrobenzyl methacrylate) spheres, nanoworms, vesicles and lamellae were reported by Zhang *et al.*[209] In this case, exposure to UV irradiation led to photoinduced cleavage of the NBMA moieties, resulting in the formation of 2-nitrobenzaldehyde and methacrylic acid residues to yield PHPMAC-P(MAA-*co*-CMA) cross-linked nanoparticles. In principle, such a hydrophobic-to-hydrophilic transition should result in nanoparticle dissolution. However, simultaneous photoinduced dimerization of the CMA moieties resulted in the formation of core cross-linked nanoparticles.

Boyer and co-workers utilized photo-PISA to prepared PEG$_{113}$-PHPMA$_y$ diblock copolymer nanoparticles via PET-RAFT aqueous dispersion polymerization.[146] Remarkably such syntheses could be conducted in the presence of air by using a water-soluble zinc *meso*-tetra(*N*-methyl-4-pyridyl)porphine tetrachloride (ZnTMPyP) photocatalyst and vitamin B$_7$ (biotin) as a singlet oxygen quencher. These reactions were

performed in a 96-well plate using red light (λ = 595 nm) at ambient temperature. Diblock copolymer spheres, worms and vesicles were prepared, with essentially full monomer conversions being achieved in all cases. Higher PHPMA DPs were required to obtain worms and vesicles using this protocol when compared to traditional thermally-initiated PISA syntheses conducted at 50 °C.[59] This is most likely because PHPMA is well-known to be slightly more hydrated at lower temperatures, thus a higher DP is required to induce nanoparticle formation. The nanoparticle cores could be modified by statistically copolymerizing HPMA with 7-[4-(trifluoromethyl)coumarin] methacrylamide (TCMAm). Importantly, the latter comonomer undergoes radical polymerization when irradiated with red light but exposure to UV light (λ = 365 nm) induces [2 + 2] cycloaddition of its coumarin-based side-chains. Nevertheless, incorporation of TCMAm did not prevent access to the full range of copolymer morphologies. Thus PEG_{113}-P(HPMA-*co*-TCMAm) spheres, worms or vesicles could be obtained via irradiation at 595 nm with cross-linking being achieved by exposure to UV light (λ = 365 nm). This new approach is a rapid and convenient strategy to prepare cross-linked nanoparticles that takes advantage of the wavelength selectivity offered by TCMAm.

In related work, Huang *et al.*[210] demonstrated the versatility of [2 + 2] cycloaddition as a cross-linking strategy by preparing $PHPMA_{40}$-$PDEMA_x$ (where DEMA = 2-((3-(4-(diethylamino)phenyl)acryloyl)oxy)ethyl methacrylate) diblock copolymer spheres, worms and vesicles by RAFT-mediated PISA in methanol. Exposure to UV light (λ = 365 nm) resulted in covalent cross-linking of the nanoparticle cores due to cycloaddition of the cinnamate functionality on the PDEMA residues. Such cross-linked nanoparticles can act as templates for the *in situ* formation of gold nanoparticles. However, this approach requires the use of specialty monomers (see **Scheme 3**) which are usually expensive or require multistep syntheses.

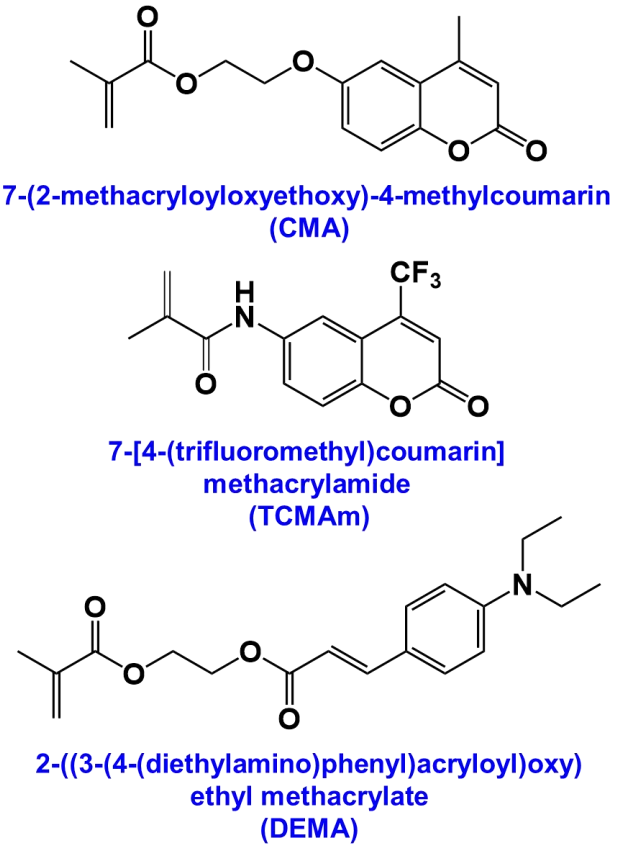

Scheme 3. Chemical structures of three vinyl monomers that undergo [2+2] cycloaddition on exposure to UV light (λ = 365 nm) to produce core core-linked nanoparticles.[146, 209-210]

Recently, Cai and co-workers reported a new strategy to crosslink vesicles and ultrathin lamellae by taking advantage of UV-activated disulfide exchange reactions.[211] The authors incorporated cystamine methacrylamide hydrochloride (CysMA) groups into nano-objects using visible light-mediated polymerization. Subsequent UV irradiation induced rapid disulfide exchange to yield covalently-stabilized nanoparticles with concomitant release of cystamine salt.

4.2 *In Situ* Cross-linking

In principle, homopolymerization of a divinyl comonomer as a third block can be a highly convenient route to cross-linked block copolymer nano-objects. However, this approach leads to a subtle change in the block copolymer composition, which may affect the copolymer morphology. This can be problematic when preparing block copolymer worms, which typically occupy relatively narrow phase space.[192] However, block copolymer vesicles can be readily cross-linked via this route with minimal change in their morphology.[193-194, 212] For example, using EGDMA as the third block enables the preparation of surfactant-

resistant PGMA-PHPMA-PEGDMA vesicles.[212] A new strategy was reported by An and co-workers in 2016, when a $PDMAC_{30}$ macro-CTA was chain-extended with DAAM plus an *asymmetric* cross-linker, allyl acrylamide (ALAM), to form covalently-stabilized block copolymer vesicles.[167] The acrylamide group in ALAM exhibits similar reactivity to that of DAAM but the allyl group reacts much more slowly; this leads to latent cross-linking in the latter stages of the PISA synthesis, i.e. well after vesicle formation. Such cross-linked vesicles were utilized as templates for the synthesis of polyelectrolyte-based vesicles via chain extension using either a cationic or anionic acrylamide comonomer.[213] X-ray photoelectron spectroscopy (XPS) confirmed that the polyelectrolytic blocks were located at the surface of the vesicles, which exhibited either positive or negative zeta potentials. Utilizing the same approach, An's group reported the synthesis of PDMA-PBzMA worms via RAFT-mediated PISA in ethanol.[214] More specifically, the statistical copolymerization of three asymmetric methacrylic cross-linkers were examined: vinyl methacrylate (VMA), allyl methacrylate (AMA) and 4-allyloxybenzyl methacrylate (ABMA), see **Scheme 4B**. Incorporating either VMA or AMA resulted in subtle morphology transitions (from pure worms to mixed phases of spheres and worms). In contrast, ABMA enabled the initial copolymer morphology to be retained. Furthermore, such cross-linked worms were obtained when using just 3% of ABMA in the nanoparticle core.

Alternatively, Pan and co-workers recently reported that *in situ* cross-linking of nanoparticles can be achieved by statistically copolymerizing a small amount of a *symmetric* bismethacrylamide comonomer (**see Scheme 4A**) with DPA. More specifically, this strategy was utilized for cross-linking PEG-P(DPA-*co*-CBMA) vesicles,[186] as discussed earlier.

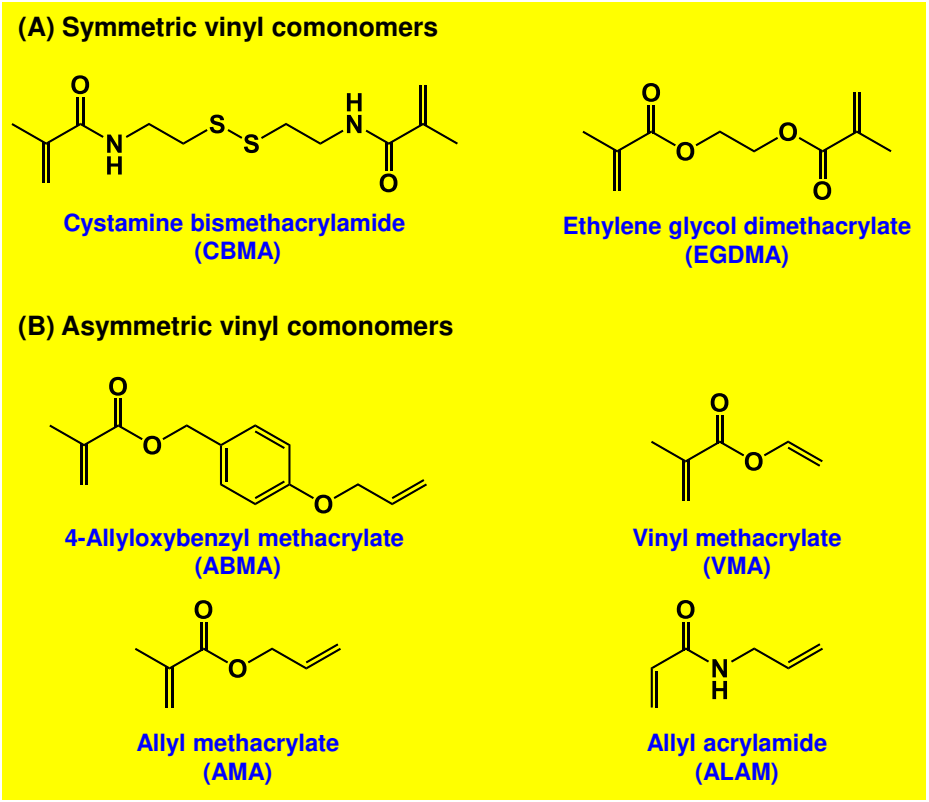

Scheme 4. Chemical structures of (A) two symmetric and (B) four asymmetric cross-linking comonomers that have been employed to prepare cross-linked block copolymer nano-objects.

The various synthetic approaches to cross-linked block copolymer nano-objects are summarized in **Table 1.** However, it is perhaps worth noting that in at least some cases such covalent stabilization may not be required. For example, amphiphilic diblock copolymer nano-objects comprising highly hydrophobic core-forming blocks such as polystyrene or poly(benzyl methacrylate) may be sufficiently stable in aqueous solution owing to the relatively strong van der Waals forces between the insoluble structure-directing chains. In such circumstances, *linear* nanoparticles can exhibit remarkable tolerance to cosolvents and/or surfactants.[215]

Table 1. Summary of the various cross-linking strategies reported in the PISA literature to prepare covalently stabilized block copolymer nano-objects.

Copolymer Composition	Solvent used for PISA synthesis	Copolymer morphology	Cross-linking reagent(s)	Reference
$PGMA_{55}$-P($HPMA_{247}$-co-$GlyMA_{82}$)	Water	Vesicles	Ethylenediamine, various Jeffamines	[194]
$PGMA_{45}$-$PGlyMA_{100}$	Water	Spheres	Ethylenediamine, PEG_{31}-diamine	[195]
PEG_{45}-$PGlyMA_y$	40:60 w/w ethanol/water	Spheres, Worms and Vesicles	Ethylenediamine	[200]
$PGMA_{56}$-P($HPMA_y$-co-$GlyMA_z$)	Water	Worms	APTES	[197]
$PGMA_{48}$–P($HPMA_{90}$-co-$GlyMA_{15}$)	Water	Long and short worms	APTES	[196]
[0.90 PEG_{113} + 0.10 $PQDMA_{125}$]-P($HPMA_{160}$-$GlyMA_{40}$)	Water	Cationic worms	APTES	[198]
[0.90 PEG_{113} + 0.10 $PQDMA_{140}$]-P($HPMA_{137}$-co-$GlyMA_{35}$)	Water	Cationic worms	MPTES	[199]
[0.90 PEG_{113} + 0.10 $PKSPMA_{111}$]-P($HPMA_{168}$-*co*-$GlyMA_{39}$)	Water	Anionic worms	MPTES	[199]
PEG_{113}-P($HPMA_x$-co-$TCMA_y$)	Water	Spheres, Worms and Vesicles	365 nm UV	[146]
$PHPMA_{40}$-$PDEMA_x$	Methanol	Spheres, Worms and Vesicles	365 nm UV	202
$PHPMAC_z$-P(MAA_x-co-CMA_y)	Water	Spheres, Worms and Vesicles	365 nm UV	[209]
$PGMA_z$-$PHPMA_x$-$PEGDMA_y$	Water	Vesicles	EGDMA	[212]

PEG_z-P(DPA_x-co-$CBMA_y$)	Water	Vesicles	CBMA	186
$PDMAC_z$-P($DAAM_x$-co-$ALAM_y$)	Water	Vesicles	ALAM	167
$PDMA_z$-P($BzMA_x$-co-$ABMA_y$)	Ethanol	Worms	ABMA	214
PSMA-PGlyMA	Mineral Oil	Spheres	*N*-methylaniline	207

5. Synthesis of Advanced Hybrid Materials by PISA

In the last 20 years, there has been increasing focus on the fabrication of hybrid nanoparticles combining organic, biological and/or inorganic components.[216-219] In principle, such nanoparticles combine the attractive properties of their constituents, which will hopefully lead to materials with synergistic performance.

5.1 Polymer/Inorganic hybrid materials by PISA

PISA enables the convenient, one-pot synthesis of polymer/inorganic hybrid nanoparticles (**Figure 9**), by either encapsulation or grafting strategies.

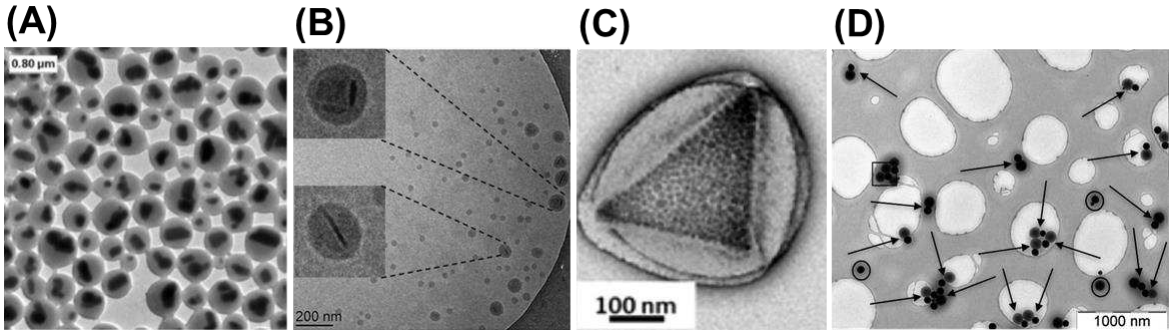

Figure 9. TEM images of various polymer/inorganic nanomaterials prepared by conducting PISA in the presence of **(A)** titanium dioxide particles (reprinted from ref [220] with permission of the American Chemical Society), **(B)** layered double hydroxides (reprinted from ref [221] with permission of The Royal Society of

Chemistry) or **(C, D)** silica nanoparticles (reprinted from ref [222] and [223], respectively with permission of the American Chemical Society). Morphologies of such hybrids can be tuned by manipulation of various parameters such as the size of the inorganic particles and the polymer/inorganic mass ratio.

For example, Hawkett's group pioneered the encapsulation of various inorganic nanoparticles via RAFT aqueous emulsion polymerization to form a diverse range of colloidal nanocomposites.[224-225] This generic approach has been exemplified for various metal oxide particles,[220, 226] carbon nanomaterials[227] and mineral platelets.[228] Bourgeat-Lami and co-workers reported a PISA formulation involving grafting from the surface of silica nanoparticles to produce a range of polymer/silica nanoparticles that exhibited multipod, snowman or tadpole-like morphologies.[229-230] In addition, Mable *et al.* demonstrated the *in situ* encapsulation of silica nanoparticles within $PGMA_{58}$-$PHPMA_{250}$ vesicles via aqueous PISA.[222] By exploiting the thermosensitive nature of these silica-loaded vesicles, the silica nanoparticles could be released on cooling to 0-5 °C as a result of a vesicle-to-sphere transition. Subsequently, the same team reported that silica nanoparticle release from similar vesicles could be modulated using dynamic covalent chemistry.[231] Such hybrid polymer/inorganic nanomaterials offer various potential applications ranging from paints and coatings[232-233] to wound repair.[234]

5.2 Polymer-protein biohybrid nano-objects by PISA

It is well-known that proteins undergo denaturation at elevated temperature,[235-237] thus the synthesis of polymer-protein conjugates via PISA requires relatively low reaction temperatures.[238-242] For example, Mable *et al*., encapsulated BSA within $PGMA_{55}$-$PHPMA_{270}$ vesicles prepared via RAFT aqueous dispersion polymerization at 37 °C [222] This reaction temperature was sufficiently low to avoid denaturation, while use of a low-temperature azo initiator generated a sufficient radical flux to ensure essentially full conversion of HPMA monomer within approximately 8 h. Similarly, Sumerlin, Zhang and co-workers encapsulated BSA within PEG-PHPMA vesicles prepared in aqueous solution via photo-PISA at 25 °C (**Figure 10A**).[107] Such mild conditions enabled more than 90% of the native activity of this enzyme to be retained. O'Reilly's group extended this photo-PISA approach to encapsulate several enzymes which retained their catalytic activity and enabled cascade reactions to be explored.[243] It is perhaps worth emphasizing here that the weakly

hydrophobic PHPMA block is partially plasticized with water, thus reagents can readily permeate the vesicle membranes, while the encapsulated enzymes are protected from proteolytic degradation.[244] Thus such enzyme-loaded vesicles may offer some potential in the context of industrial biotechnology. More recently, O'Reilly's group has also shown that using an appropriate surfactant enables the insertion of membrane proteins within vesicle membranes during their formation via photo-PISA (**Figure 10B**).[245] Perhaps surprisingly, proteins can also be employed as steric stabilizers during PISA to produce unique, self-assembled protein-polymer nanoparticles (**Figure 10C**).

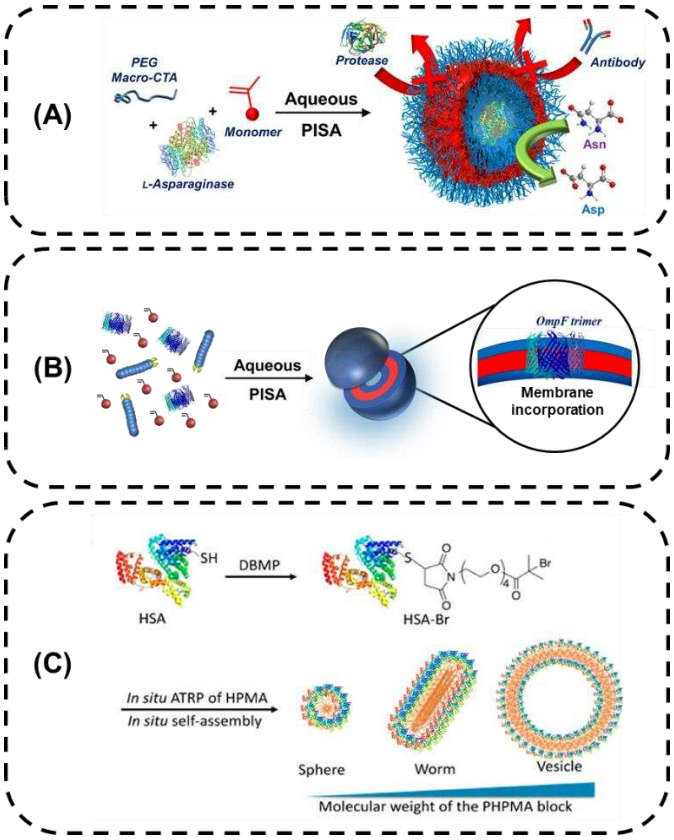

Figure 10. Synthesis of various protein-polymer nanoparticles by aqueous PISA. Proteins can be **(A)** encapsulated within vesicles (reprinted from ref [244] with permission of the American Chemical Society), **(B)** introduced within vesicle membranes to control the selective transport of small molecules (adapted from ref [245] with permission of the American Chemical Society or **(C)** used as a reactive steric stabilizer to prepare protein-stabilized nanoparticles (reprinted from ref [121] with permission of the American Chemical Society).

This approach was first reported by Gao and Liu, who polymerized HPMA directly from human serum albumin (HSA), which was modified with an ATRP initiator group at its cysteine-34 site.[121] Depending on the precise reaction conditions, HSA-PHPMA$_x$ spheres, worms or vesicles could be synthesized in aqueous solution. In each case, almost complete retention of HSA esterase activity was observed compared to the free protein. This approach was also later exploited for increasing the blood circulation half-life of interferon-α, a promising cytokine with a range of potent biological responses.[246] More recently, Huang and co-workers employed a PET-RAFT strategy to polymerize HPMA from a RAFT agent-functionalized BSA precursor, and demonstrated that encapsulated therapeutics could be released in the presence of proteases.[247]

6. Improved throughput during PISA

RAFT polymerization involves radical species and hence is sensitive to retardation in the presence of oxygen.[248] Thus PISA syntheses are routinely conducted using deoxygenated reaction solutions, usually achieved via freeze-pump-thaw cycles or by degassing using an insert gas (N_2 or Argon). However, such protocols increase the complexity of PISA syntheses and significantly increase the difficulty to conduct high-throughput experiments using small volumes (μL). If this limitation could be addressed, it could enable rapid optimization of reaction conditions via parallel experimentation.

In principle, PISA syntheses can be performed under a nitrogen atmosphere using an automated synthesizer unit.[249-250] This approach was recently demonstrated by Cockram and co-workers, who used a Chemspeed AutoPlant A100 synthesizer to perform up to 20 simultaneous RAFT aqueous emulsion polymerizations (**Figure 11A**).

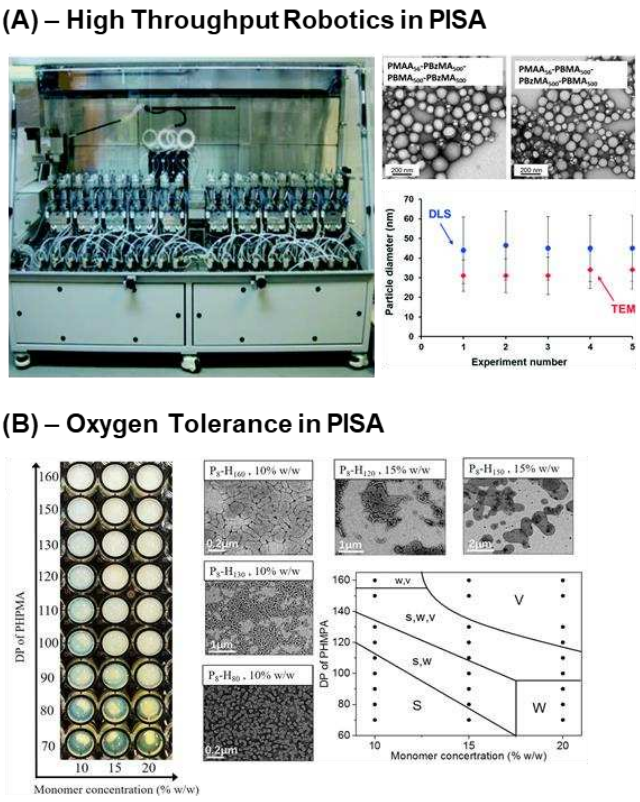

Figure 11. Implementation of **(A)** automated robotic synthesizers (adapted from ref [251] with permission of the Royal Society of Chemistry) and **(B)** oxygen tolerant, high throughput strategies (adapted from ref [252] with permission of the American Chemical Society) for the acceleration of materials discovery in the context of new PISA formulations.

Using mechanical stirring, either PMAA-PBuMA (where PBuMA = poly(*n*-butyl methacrylate) or PMAA-PBzMA spheres could be obtained with high reproducibility at up to 45 % w/w solids. Such syntheses resulted in relatively broad molecular weight distributions, but blocking efficiencies remained sufficiently high to enable the synthesis of colloidally stable tetrablock copolymer nanoparticles.

As an alternative to robotic/automated synthesizers, oxygen inhibition can be minimized by conducting *chemical* deoxygenation of reaction mixtures using either enzymes or photochemistry.[253-257] This can facilitate parallel syntheses without requiring specialized equipment. Furthermore, polymerizations can be conducted at microlitre (or even smaller) scales, thus improving the efficiency of high-throughput PISA.[258] Chemical deoxygenation was first reported by Boyer and co-workers, who employed a photocatalyst to convert molecular oxygen into singlet oxygen, with the latter species being trapped using a suitable quencher.[259-260] Subsequently, the same team demonstrated that oxygen-tolerant photoinitiation enabled

PISA syntheses to be conducted directly in 96-well microliter plates, enabling the convenient parallel synthesis of self-assembled nanoparticles on a laboratory benchtop.[261] In addition, Tan's group[112, 252] demonstrated that PISA syntheses could be conducted by utilizing the enzyme deoxygenation approach.[258] Using this strategy, a phase diagram was rapidly constructed by performing multiple PISA syntheses in a single pass, although the subsequent morphology assignments presumably remain a bottleneck (**Figure 11B**). More recently, Gianneschi and co-workers have developed a high throughput TEM method using automated TEM and automated image analysis to rapidly generate phase diagrams, which removes one of the main limitations in the characterization of PISA samples.[262] In summary, recent advances in high throughput PISA syntheses and characterization methods hold considerable promise for accelerating the pace of materials discovery and optimization of nanoparticle formulations.

7. PISA under Continuous Flow for Scalable Synthesis

Compared to traditional block copolymer self-assembly strategies, PISA can be performed at much higher solids. In some cases, colloidally stable nanoparticles can be prepared at copolymer concentrations of up to 50% w/w,[28] which augurs well for the industrial scale-up of PISA formulations. In this context, continuous flow syntheses are becoming increasingly favored over batch syntheses,[263] as it offers superior heat/mass transfer, enhanced reaction rates and the potential for integrated feedback control loops.[264-266] Zhu and co-workers reported the first example of PISA conducted under continuous flow conditions, where methyl methacrylate (MMA) was polymerized from a PEGMA macro-CTA in a stainless steel tubular reactor via thermally-initiated RAFT emulsion polymerization (**Figure 12A**).[267]

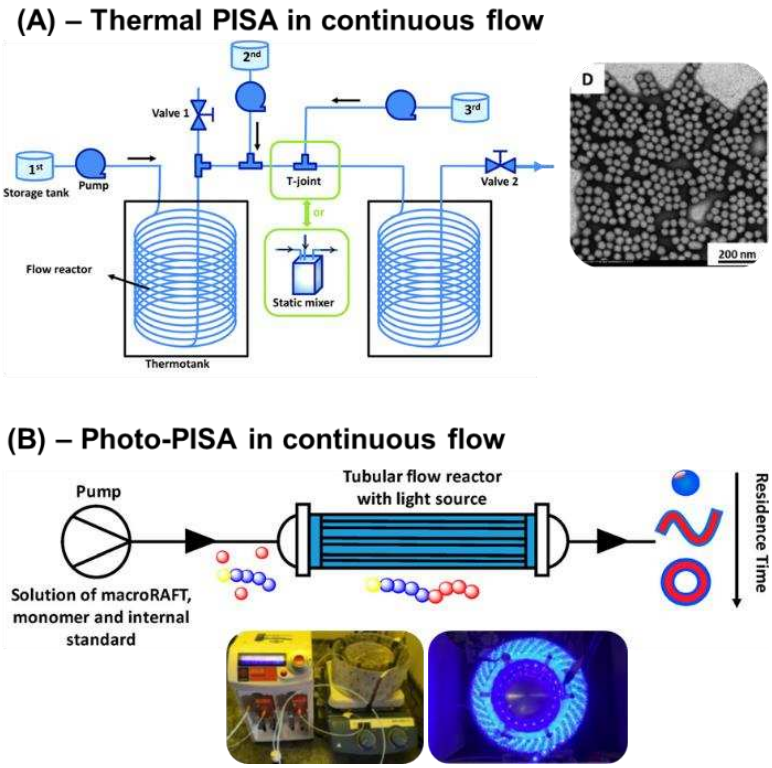

Figure 12. RAFT-mediated PISA syntheses performed under continuous flow conditions using **(A)** thermal initiation (adapted from ref [267] with permission from the Royal Society of Chemistry) and **(B)** photoinitiation (adapted from ref [268] with permission from the American Chemical Society). Such advances augur well for the eventual industrial scale-up of PISA.

Using a two-stage flow process, amphiphilic diblock copolymer spheres could be prepared with adjustable mean diameters. Recently, Warren and coworkers applied an all-aqueous continuous flow approach for the synthesis of PDMAC-PDAAM nanoparticles.[269] Using a 5 mL stainless steel coil reactor resulted in significantly faster kinetics compared to a batch process, which was attributed to the increased heat transfer in the tubular reactor. Furthermore, higher order morphologies such as worms and vesicles could also be readily synthesized under these continuous flow conditions at concentrations as high as 20 wt%.

Recently, a team led by Boyer, Junkers and Zetterlund developed an alternative approach: photopolymerization was used to initiate aqueous PISA to convert a batch reaction into a continuous flow process.[268, 270-271] Photopolymerization under flow conditions significantly reduces the problem of light intensity gradients (or light diffusion) encountered for batch processes owing to internal absorption effects.[272] Leveraging this advantage, a prototype microflow photoreactor (1 mm inner diameter) was

developed that was capable of producing up to 60 g of a desired nanoparticle morphology in a single day (**Figure 12B**). Furthermore, the mild photopolymerization conditions enabled the *in situ* encapsulation of a well-known anticancer drug (doxorubicin) during the PISA process. Although the full potential of continuous flow PISA syntheses are yet to be fully realized, this chemical engineering approach holds significant promise for the successful implementation of PISA on a commercially viable scale.

8. Conclusions and Prospects

In recent years, the PISA landscape has evolved significantly with the introduction of a plethora of new chemical tools for the synthesis and characterization of PISA-derived nanoparticles. For example, a wide range of new initiation methods have been developed as alternatives to thermally initiated RAFT polymerization over the past five years. Some of these photochemical,[33] enzymatic,[90] ultrasonic[118] or even radiochemical[119] techniques have shown that PISA can be achieved under a much broader range of experimental conditions than previously demonstrated. For example, these advances have enabled the efficient and rapid synthesis of vesicles at close to room temperature, allowing the *in situ* encapsulation of thermally-sensitive therapeutics such as small-molecule drugs,[268] proteins[107] and even nucleic acids[247] without affecting their bioactivities. Such loading strategies are expected to have a significant impact in the field of drug delivery by providing an efficient route for the direct encapsulation of sensitive biological therapeutics. More recently, Cai and co-workers have proposed a liquid-liquid separation mode via PISA, utilizing liquid coacervate droplets and photo-PISA.[273] This approach could be used for the encapsulation of therapeutic compounds (such as siRNA, DNA, and other biomolecules) via electrostatic interactions using the liquid coacervate droplets as reservoirs.

In addition to new initiation methods, various alternative RDRP techniques have been utilized for PISA syntheses. Techniques such as NMP,[122] ATRP,[67, 120] iodine-mediated polymerization (ITP)[126-127] and even sulfur-free RAFT[128-129] may be preferable for their ability to produce non-colored nanoparticles without malodorous or potentially toxic sulfur-based residues. Additionally, these strategies produce copolymers with chemically diverse chain-ends, which may enable an even broader toolbox of post-polymerization

techniques to be applied. Beyond radical-based polymerization, techniques evoking ionic polymerization and especially ROMP-based strategies continue to broaden the PISA field, enabling the design of self-assembled nanomaterials with new monomer families. Such discoveries will be likely aided by *in silico* predictions of monomer behavior in PISA as recently demonstrated by O'Reilly's group.[274-275] Further, such strategies may be more compatible with certain therapeutic drugs that might be otherwise difficult to integrate into a radical-based synthesis. For example, Delaittre's group recently demonstrated a protecting group-free, one-pot synthesis of nitroxide radical-functionalized polymeric nanoparticles using ROMP PISA to circumvent issues using radical based polymerization.[276] In addition, these techniques may lead to the design of biodegradable polymeric nanoparticles for drug delivery applications. Indeed, the morphology of nanoparticles can have a significant effect on their biodistribution, as well as their interaction with (and accumulation within) different cells.[277-280] Designing fully biodegradable nanoparticles with well-defined morphology could have a significant impact in anti-cancer treatment and provide further understanding into their *in vivo* biodistribution.

There is also increasing interest in the use of external stimuli to provide fine control over the size and shape of PISA-derived nanoparticles. For example, light has been harnessed to provide spatiotemporal control over initiation,[24] crosslinking[209] and/or to modify the hydrophobic/hydrophilic block ratio.[281] Furthermore, the potential to activate differing chemical processes using two or more wavelengths of UV/visible light (or alternative stimuli) opens up the possibility of performing orthogonal reactions such as on-demand crosslinking during PISA.[178] In principle, this approach could provide access to unusual morphologies owing to stepwise changes in copolymer chain mobility. For example, fabrication of core/corona compartmentalized nanoparticles could be useful drug delivery because it may enable (i) simultaneous encapsulation of multiple therapeutic agents, (ii) the stabilization of polymer blends or (iii) the production of hybrid organic/inorganic nanoparticles.[282-283] For example, Tan and co-workers recently reported the use of photo-PISA to prepare so-called 'patchy' worms by chain extension of crosslinked polymeric nanoparticles.[284]

Apart from the introduction of new chemistries, various engineering approaches have been developed to increase the rate at which block copolymer nanoparticles can be synthesized via PISA. A recent pilot study

has already demonstrated the feasibility of implementing automated synthesizers (with inert working environments) for high-throughput PISA syntheses.[251] As an alternative, inherently oxygen-tolerant polymerization protocols have also been developed which may be more attractive for conducting high-throughput PISA in an academic setting because they do not require any specialized equipment.[252, 261] In principle, these high-throughput strategies enable rapid optimization of PISA formulations: this is particularly relevant given the large number of reaction variables (monomer concentration, target degree of polymerization, temperature, solvent composition, etc.) affecting the self-assembly process. Furthermore, this approach provides a versatile synthesis platform to implement structure-activity screening approaches similar to those already used in the pharmaceutical and drug discovery industries.[285] PISA formulations have also recently been examined in the context of continuous flow reactors, allowing rapid manufacturing of relatively large quantities of block copolymer nanoparticles with a precise morphology.[269] [268] Such an engineering approach can significantly improve the overall yield of polymeric nanomaterials compared to that achieved using batch reactors without some of the issues of scale associated with the latter approach, such as poor heat transfer and irreproducibility between batch reactions.[286] Currently, there is little known regarding the potential effect of shear and nanoparticle-induced changes in solution viscosity during nanoparticle formation under confined flow conditions. It seems likely that computational fluid dynamics could be of significant utility in this context. In addition, combining flow PISA processes with *in situ* encapsulation of therapeutic agents could facilitate rapid production of drug-loaded nanoparticles for biomedical applications. Finally, the implementation of PISA under continuous flow conditions should facilitate integration of online monitoring techniques, which could provide an elegant solution for improving the reproducibility of the PISA process.[287]

Author Information

[†]N.J.W.P and J.Y. both contributed equally in the preparation of this manuscript.

*Corresponding authors e-mail: s.p.armes@sheffield.ac.uk, cboyer@unsw.edu.au

ORCID

Nicholas J. W. Penfold: 0000-0002-6505-3782

Jonathan Yeow: 0000-0003-3709-5149

Cyrille Boyer: 0000-0002-4564-4702

Steven P. Armes: 0000-0002-8289-6351

Acknowledgements

S.P.A. acknowledges the EPSRC for an Established Career Particle Technology Fellowship (EP/R003009), which provided postdoctoral support for N.J.W.P. C.B thanks the Australian Research Council for his Future Fellowship (FT12010096).

List of Abbreviations

Full Chemical Name	Abbreviation
2-(Diethylamino)ethyl methacrylate	DEA
2-(Dimethylamino)ethyl methacrylate	DMAEMA
2-Ethoxyethyl methacrylate	EEMA
2-Hydroxypropyl methacrylate	HPMA
2-Methoxyethyl acrylate	MEA
2-Nitrobenzyl methacrylate	NBMA
3-(Benzylthiocarbonothioylthio) propanoic acid	BTPA
3-Aminopropylsiloxane	APTES
3-Mercaptopropylsiloxane	MPTES
4-Allyloxybenzyl Methacrylate	ABMA
7-(2-Methacryloyloxyethoxy)-4-methylcoumarin	CMA
7-[4-(Trifluoromethyl)coumarin] methacrylamide	TCMAm
Addition-fragmentation chain transfer	AFCT
Adipic dihydrazide	ADH
Allyl acrylamide	ALAM
Allyl methacrylate	AMA
Atom transfer radical polymerization	ATRP
Bovine serum albumin	BSA
Controlled/living radical polymerization	CLRP
Critical gelation temperature	CGT
Crystallization-driven self-assembly	CDSA
Cystamine bismethacrylamide	CBMA
Degree of polymerization	DP
Di(ethylene glycol) methyl ether methacrylate	DEGMA
Diacetone acrylamide	DAAM
Dynamic light scattering	DLS
Ethylene glycol dimethacrylate	EGDMA

Glucose oxidase	GOX
Glycidyl methacrylate	GlyMA
Horseradish peroxidase	HRP
Human serum albumin	HSA
Initiators for continuous activator regeneration	ICAR
Iodine-mediated polymerization	ITP
Light emitting diode	LED
Lower critical solution temperature	LCST
Macromolecular chain-transfer agent	macro-CTA
Methacrylic acid	MAA
Methyl methacrylate	MMA
N,N-Diethylacrylamide	DEAA
N,N-Dimethylformamide	DMF
N-Isopropylacrylamide	NIPAM
Nitroxide-mediated polymerization	NMP
Nuclear magnetic resonance	NMR
Photoinduced electron/energy transfer-reversible addition-fragmentation chain transfer	PET-RAFT
Poly((2-methacryloyloxy)ethyl phosphoryl-choline)	PMPC
Poly(2-(diisopropylamino)ethyl methacrylate)	PDPA
Poly(2-(methylthio)ethyl methacrylate	PMTEMA
Poly(benzyl methacrylate)	PBzMA
Poly(glycerol monomethacrylate)	PGMA
Poly(lauryl methacrylate)	PLMA
Poly(*N*-(2-methacryloyloxy)ethyl pyrrolidone	PNMEP
Poly(*N,N*-dimethyl acrylamide)	PDMAC
Poly(*N*-acryloylmorpholine)	PNAM
Poly(*N*-acryloylthiomorpholine)	PNAT
Poly(*n*-butyl methacrylate)	PBuMA
Poly(oligo(ethylene glycol) methyl ether methacrylate	POEGMA
Poly(phenyl acrylate)	PPhA
Poly(poly(ethylene glycol) methyl ether methacrylate	PPEGMA
Poly(stearyl methacrylate)	PSMA
Polymerization-induced self-assembly	PISA
Reversible addition-fragmentation chain transfer	RAFT
Reversible deactivation radical polymerization	RDRP
Ring-opening metathesis polymerization	ROMP
Scanning electron microscopy	SEM
Small angle X-ray scattering	SAXS
Sodium phenyl-2, 4, 6-trimethylbenzoylphosphinate	SPTP
t-Butyl acrylate	*t*BA
Transmission electron microscopy	TEM
Upper critical solution temperature	UCST
Vinyl methacrylate	VMA

References

1. Bates, F. S., Polymer-polymer phase behavior. *Science* **1991,** *251* (4996), 898-905.

2. Khandpur, A. K.; Foerster, S.; Bates, F. S.; Hamley, I. W.; Ryan, A. J.; Bras, W.; Almdal, K.; Mortensen, K., Polyisoprene-Polystyrene Diblock Copolymer Phase Diagram near the Order-Disorder Transition. *Macromolecules* **1995,** *28* (26), 8796-806.

3. Bates, F. S.; Fredrickson, G. H., Block copolymers-designer soft materials. *Physics Today* **1999,** *52* (2), 32-38.

4. Mai, Y.; Eisenberg, A., Self-assembly of block copolymers. *Chem. Soc. Rev.* **2012,** *41* (18), 5969-85.

5. Discher, D. E.; Eisenberg, A., Materials science: Soft surfaces: Polymer vesicles. *Science* **2002,** *297* (5583), 967-973.

6. Discher, B. M.; Won, Y.-Y.; Ege, D. S.; Lee, J. C. M.; Bates, F. S.; Discher, D. E.; Hammer, D. A., Polymersomes: Tough vesicles made from diblock copolymers. *Science* **1999,** *284* (5417), 1143-1146.

7. Won, Y.-Y.; Davis, H. T.; Bates, F. S., Giant wormlike rubber micelles. *Science* **1999,** *283* (5404), 960-963.

8. Gohy, J.-F.; Lohmeijer, B. G. G.; Alexeev, A.; Wang, X.-S.; Manners, I.; Winnik, M. A.; Schubert, U. S., Cylindrical micelles from the aqueous self-assembly of an amphiphilic poly(ethylene oxide)-b-poly(ferrocenylsilane) (PEO-b-PFS) block copolymer with a metallo-supramolecular linker at the block junction. *Chem. A Eur. J.* **2004,** *10* (17), 4315-4323.

9. Gilroy, J. B.; Gaedt, T.; Whittell, G. R.; Chabanne, L.; Mitchels, J. M.; Richardson, R. M.; Winnik, M. A.; Manners, I., Monodisperse cylindrical micelles by crystallization-driven living self-assembly. *Nat. Chem.* **2010,** *2* (7), 566-570.

10. Jang, S. G.; Audus, D. J.; Klinger, D.; Krogstad, D. V.; Kim, B. J.; Cameron, A.; Kim, S.-W.; Delaney, K. T.; Hur, S.-M.; Killops, K. L.; Fredrickson, G. H.; Kramer, E. J.; Hawker, C. J., Striped, Ellipsoidal Particles by Controlled Assembly of Diblock Copolymers. *J. Am. Chem. Soc.* **2013,** *135* (17), 6649-6657.

11. Pochan, D. J.; Chen, Z.; Cui, H.; Hales, K.; Qi, K.; Wooley, K. L., Toroidal Triblock Copolymer Assemblies. *Science* **2004,** *306* (5693), 94-97.

12. Zhang, L.; Eisenberg, A., Multiple morphologies of "crew-cut" aggregates of polystyrene-b-poly(acrylic acid) block copolymers. *Science* **1995,** *268* (5218), 1728-1731.

13. Shen, H.; Zhang, L.; Eisenberg, A., Thermodynamics of crew-cut micelle formation of polystyrene-b-poly(acrylic acid) diblock copolymers in DMF/H2O mixtures. *J. Phys. Chem. B* **1997,** *101* (24), 4697-4708.

14. Zhang, L.; Shen, H.; Eisenberg, A., Phase Separation Behavior and Crew-Cut Micelle Formation of Polystyrene-b-poly(acrylic acid) Copolymers in Solutions. *Macromolecules* **1997,** *30* (4), 1001-1011.

15. Yu, K.; Eisenberg, A., Bilayer Morphologies of Self-Assembled Crew-Cut Aggregates of Amphiphilic PS-b-PEO Diblock Copolymers in Solution. *Macromolecules* **1998,** *31* (11), 3509-3518.

16. Liu, F.; Eisenberg, A., Preparation and pH Triggered Inversion of Vesicles from Poly(acrylic Acid)-block-Polystyrene-block-Poly(4-vinyl Pyridine). *J. Am. Chem. Soc.* **2003,** *125* (49), 15059-15064.

17. Soo, P. L.; Eisenberg, A., Preparation of block copolymer vesicles in solution. *J. Polym. Sci., Part A: Polym. Chem.* **2004,** *42* (6), 923-938.

18. Warren, N. J.; Armes, S. P., Polymerization-induced self-assembly of block copolymer nano-objects via RAFT aqueous dispersion polymerization. *J. Am. Chem. Soc.* **2014,** *136* (29), 10174-10185.

19. Canning, S. L.; Smith, G. N.; Armes, S. P., A Critical Appraisal of RAFT-Mediated Polymerization-Induced Self-Assembly. *Macromolecules* **2016,** *49* (6), 1985-2001.

20. Derry, M. J.; Fielding, L. A.; Armes, S. P., Polymerization-induced self-assembly of block copolymer nanoparticles via RAFT non-aqueous dispersion polymerization. *Prog. Polym. Sci.* **2016,** *52*, 1-18.

21. Rieger, J., Guidelines for the Synthesis of Block Copolymer Particles of Various Morphologies by RAFT Dispersion Polymerization. *Macromol. Rapid Commun.* **2015,** *36* (16), 1458-1471.

22. Pei, Y.; Lowe, A. B.; Roth, P. J., Stimulus-Responsive Nanoparticles and Associated (Reversible) Polymorphism via Polymerization Induced Self-assembly (PISA). *Macromol. Rapid Commun.* **2017,** *38* (1), 1600528.

23. Lowe, A. B., RAFT alcoholic dispersion polymerization with polymerization-induced self-assembly. *Polymer* **2016,** *106*, 161-181.

24. Yeow, J.; Boyer, C., Photoinitiated Polymerization-Induced Self-Assembly (Photo-PISA): New Insights and Opportunities. *Adv. Sci.* **2017,** *4* (7), 1700137.

25. Charleux, B.; Delaittre, G.; Rieger, J.; D'Agosto, F., Polymerization-Induced Self-Assembly: From Soluble Macromolecules to Block Copolymer Nano-Objects in One Step. *Macromolecules* **2012,** *45* (17), 6753-6765.

26. Foster, J. C.; Varlas, S.; Couturaud, B.; Coe, Z.; O'Reilly, R. K., Getting into Shape: Reflections on a New Generation of Cylindrical Nanostructures' Self-Assembly Using Polymer Building Blocks. *J. Am. Chem. Soc.* **2019,** *141* (7), 2742-2753.

27. Cunningham, V. J.; Alswieleh, A. M.; Thompson, K. L.; Williams, M.; Leggett, G. J.; Armes, S. P.; Musa, O. M., Poly(glycerol monomethacrylate)-poly(benzyl methacrylate) diblock copolymer nanoparticles via RAFT emulsion polymerization: Synthesis, characterization, and interfacial activity. *Macromolecules* **2014,** *47* (16), 5613-5623.

28. Derry, M. J.; Fielding, L. A.; Armes, S. P., Industrially-relevant polymerization-induced self-assembly formulations in non-polar solvents: RAFT dispersion polymerization of benzyl methacrylate. *Polym. Chem.* **2015,** *6* (16), 3054-3062.

29. Blanazs, A.; Madsen, J.; Battaglia, G.; Ryan, A. J.; Armes, S. P., Mechanistic insights for block copolymer morphologies: how do worms form vesicles? *J. Am. Chem. Soc.* **2011,** *133* (41), 16581-16587.

30. Chaduc, I.; Girod, M.; Antoine, R.; Charleux, B.; D'Agosto, F.; Lansalot, M., Batch Emulsion Polymerization Mediated by Poly(methacrylic acid) MacroRAFT Agents: One-Pot Synthesis of Self-Stabilized Particles. *Macromolecules* **2012,** *45* (15), 5881-5893.

31. Blanazs, A.; Verber, R.; Mykhaylyk, O. O.; Ryan, A. J.; Heath, J. Z.; Douglas, C. W.; Armes, S. P., Sterilizable gels from thermoresponsive block copolymer worms. *J. Am. Chem. Soc.* **2012,** *134* (23), 9741-9748.

32. Byard, S. J.; Williams, M.; McKenzie, B. E.; Blanazs, A.; Armes, S. P., Preparation and Cross-Linking of All-Acrylamide Diblock Copolymer Nano-Objects via Polymerization-Induced Self-Assembly in Aqueous Solution. *Macromolecules* **2017,** *50*, 1482-1493.

33. Jiang, Y.; Xu, N.; Han, J.; Yu, Q.; Guo, L.; Gao, P.; Lu, X.; Cai, Y., The direct synthesis of interface-decorated reactive block copolymer nanoparticles via polymerisation-induced self-assembly. *Polym. Chem.* **2015,** *6* (27), 4955-4965.

34. Shen, W.; Chang, Y.; Liu, G.; Wang, H.; Cao, A.; An, Z., Biocompatible, Antifouling, and Thermosensitive Core−Shell Nanogels Synthesized by RAFT Aqueous Dispersion Polymerization. *Macromolecules* **2011,** *44* (8), 2524-2530.

35. Grazon, C.; Rieger, J.; Sanson, N.; Charleux, B., Study of poly(N,N-diethylacrylamide) nanogel formation by aqueous dispersion polymerization of N,N-diethylacrylamide in the presence of poly(ethylene oxide)-b-poly(N,N-dimethylacrylamide) amphiphilic macromolecular RAFT agents. *Soft Matt.* **2011,** *7* (7), 3482-3490.

36. Semsarilar, M.; Penfold, N. J. W.; Jones, E. R.; Armes, S. P., Semi-crystalline diblock copolymer nano-objects prepared via RAFT alcoholic dispersion polymerization of stearyl methacrylate. *Polym. Chem.* **2015,** *6*, 1751-1757.

37. Pei, Y.; Dharsana, N. C.; Lowe, A. B., Ethanolic RAFT dispersion polymerization of 2-(naphthalen-2-yloxy)ethyl methacrylate and 2-phenoxyethyl methacrylate with poly[2-(dimethylamino)ethyl methacrylate] macro-chain transfer agents. *Aust. J. Chem.* **2015,** *68* (6), 939-945.

38. Pei, Y.; Dharsana, N. C.; van Hensbergen, J. A.; Burford, R. P.; Roth, P. J.; Lowe, A. B., RAFT dispersion polymerization of 3-phenylpropyl methacrylate with poly[2-(dimethylamino)ethyl methacrylate] macro-CTAs in ethanol and associated thermoreversible polymorphism. *Soft Matt.* **2014,** *10* (31), 5787-5796.

39. Pei, Y.; Lowe, A. B., Polymerization-induced self-assembly: ethanolic RAFT dispersion polymerization of 2-phenylethyl methacrylate. *Polym. Chem.* **2014,** *5* (7), 2342-2351.

40. Jones, E. R.; Semsarilar, M.; Blanazs, A.; Armes, S. P., Efficient Synthesis of Amine-Functional Diblock Copolymer Nanoparticles via RAFT Dispersion Polymerization of Benzyl Methacrylate in Alcoholic Media. *Macromolecules* **2012,** *45* (12), 5091-5098.

41. Jones, E. R.; Semsarilar, M.; Wyman, P.; Boerakker, M.; Armes, S. P., Addition of water to an alcoholic RAFT PISA formulation leads to faster kinetics but limits the evolution of copolymer morphology. *Polym. Chem.* **2016,** *7* (4), 851-859.

42. Fielding, L. A.; Derry, M. J.; Ladmiral, V.; Rosselgong, J.; Rodrigues, A. M.; Ratcliffe, L. P. D.; Sugihara, S.; Armes, S. P., RAFT dispersion polymerization in non-polar solvents: facile production of block copolymer spheres, worms and vesicles in n-alkanes. *Chem. Sci.* **2013,** *4* (5), 2081-2087.

43. Fielding, L. A.; Lane, J. A.; Derry, M. J.; Mykhaylyk, O. O.; Armes, S. P., Thermo-responsive diblock copolymer worm gels in non-polar solvents. *J. Am. Chem. Soc.* **2014,** *136* (15), 5790-5798.

44. Houillot, L.; Bui, C.; Save, M.; Charleux, B.; Farcet, C.; Moire, C.; Raust, J.-A.; Rodriguez, I., Synthesis of Well-Defined Polyacrylate Particle Dispersions in Organic Medium Using Simultaneous RAFT Polymerization and Self-Assembly of Block Copolymers. A Strong Influence of the Selected Thiocarbonylthio Chain Transfer Agent. *Macromolecules* **2007,** *40* (18), 6500-6509.

45. Pei, Y.; Thurairajah, L.; Sugita, O. R.; Lowe, A. B., RAFT dispersion polymerization in nonpolar media: Polymerization of 3-phenylpropyl methacrylate in n-tetradecane with poly(stearyl methacrylate) homopolymers as macro chain transfer agents. *Macromolecules* **2015,** *48* (1), 236-244.

46. Lopez-Oliva, A. P.; Warren, N. J.; Rajkumar, A.; Mykhaylyk, O. O.; Derry, M. J.; Doncom, K. E. B.; Rymaruk, M. J.; Armes, S. P., Polydimethylsiloxane-based diblock copolymer nano-objects prepared in nonpolar media via raft-mediated polymerization-induced self-assembly. *Macromolecules* **2015,** *48* (11), 3547-3555.

47. Zhang, Q.; Zhu, S., Ionic liquids: Versatile media for preparation of vesicles from polymerization-induced self-assembly. *ACS Macro Lett.* **2015,** *4* (7), 755-758.

48. Rymaruk, M. J.; Hunter, S. J.; O'Brien, C. T.; Brown, S. L.; Williams, C. N.; Armes, S. P., RAFT Dispersion Polymerization in Silicone Oil. *Macromolecules* **2019,** *52* (7), 2822-2832.

49. Hasell, T.; Thurecht, K. J.; Jones, R. D.; Brown, P. D.; Howdle, S. M., Novel one pot synthesis of silver nanoparticle-polymer composites by supercritical CO2 polymerisation in the presence of a RAFT agent. *Chem. Commun.* **2007,** (38), 3933-5.

50. Zong, M.; Thurecht, K. J.; Howdle, S. M., Dispersion polymerisation in supercritical CO2 using macro-RAFT agents. *Chem. Commun.* **2008,** (45), 5942-5944.

51. Xu, A.; Lu, Q.; Huo, Z.; Ma, J.; Geng, B.; Azhar, U.; Zhang, L.; Zhang, S., Synthesis of fluorinated nanoparticles via RAFT dispersion polymerization-induced self-assembly using fluorinated macro-RAFT agents in supercritical carbon dioxide. *RSC Adv.* **2017,** *7* (81), 51612-51620.

52. Zhou, D.; Kuchel, R. P.; Dong, S.; Lucien, F. P.; Perrier, S.; Zetterlund, P. B., Polymerization-Induced Self-Assembly under Compressed CO2 : Control of Morphology Using a CO2 -Responsive MacroRAFT Agent. *Macromol. Rapid Commun.* **2019,** *40* (2), e1800335.

53. Dong, S.; Zhao, W.; Lucien, F. P.; Perrier, S.; Zetterlund, P. B., Polymerization induced self-assembly: tuning of nano-object morphology by use of CO2. *Polym. Chem.* **2015,** *6* (12), 2249-2254.

54. Jenkins, A. D.; Kratochvil, P.; Stepto, R. F. T.; Suter, U. W., Glossary of basic terms in polymer science. *Pure Appl. Chem.* **1996,** *68* (12), 2287-2311.

55. Blanazs, A.; Ryan, A. J.; Armes, S. P., Predictive Phase Diagrams for RAFT Aqueous Dispersion Polymerization: Effect of Block Copolymer Composition, Molecular Weight, and Copolymer Concentration. *Macromolecules* **2012,** *45* (12), 5099-5107.

56. Penfold, N. J. W.; Whatley, J. R.; Armes, S. P., Thermoreversible Block Copolymer Worm Gels Using Binary Mixtures of PEG Stabilizer Blocks. *Macromolecules* **2019,** *52* (4), 1653-1662.

57. Li, X.; Gao, Y.; Boott, C. E.; Hayward, D. W.; Harniman, R.; Whittell, G. R.; Richardson, R. M.; Winnik, M. A.; Manners, I., "Cross" Supermicelles via the Hierarchical Assembly of Amphiphilic Cylindrical Triblock Comicelles. *J. Am. Chem. Soc.* **2016,** *138* (12), 4087-4095.

58. Blackman, L. D.; Doncom, K. E. B.; Gibson, M. I.; O'Reilly, R. K., Comparison of photo- and thermally initiated polymerization-induced self-assembly: a lack of end group fidelity drives the formation of higher order morphologies. *Polym. Chem.* **2017,** *8*, 2860-2871.

59. Warren, N. J.; Mykhaylyk, O. O.; Mahmood, D.; Ryan, A. J.; Armes, S. P., RAFT aqueous dispersion polymerization yields poly(ethylene glycol)-based diblock copolymer nano-objects with predictable single phase morphologies. *J. Am. Chem. Soc.* **2014,** *136* (3), 1023-1033.

60. Gonzato, C.; Semsarilar, M.; Jones, E. R.; Li, F.; Krooshof, G. J. P.; Wyman, P.; Mykhaylyk, O. O.; Tuinier, R.; Armes, S. P., Rational Synthesis of Low-Polydispersity Block Copolymer Vesicles in

Concentrated Solution via Polymerization-Induced Self-Assembly. *J. Am. Chem. Soc.* **2014,** *136* (31), 11100-11106.

61. Mable, C. J.; Fielding, L. A.; Derry, M. J.; Mykhaylyk, O. O.; Chambon, P.; Armes, S. P., Synthesis and pH-responsive dissociation of framboidal ABC triblock copolymer vesicles in aqueous solution. *Chem. Sci.* **2018,** *9* (6), 1454-1463.

62. Mable, C. J.; Warren, N. J.; Thompson, K. L.; Mykhaylyk, O. O.; Armes, S. P., Framboidal ABC triblock copolymer vesicles: a new class of efficient pickering emulsifier. *Chem. Sci.* **2015,** *6* (11), 6179-6188.

63. Wang, X.; Zhou, J.; Lv, X.; Zhang, B.; An, Z., Temperature-Induced Morphological Transitions of Poly(dimethylacrylamide)-Poly(diacetone acrylamide) Block Copolymer Lamellae Synthesized via Aqueous Polymerization-Induced Self-Assembly. *Macromolecules* **2017,** *50* (18), 7222-7232.

64. Yang, P.; Ratcliffe, L. P. D.; Armes, S. P., Efficient synthesis of poly(methacrylic acid)-block-poly(styrene-alt-n phenylmaleimide) diblock copolymer lamellae using RAFT dispersion polymerization. *Macromolecules* **2013,** *46* (21), 8545-8556.

65. Yang, P.; Mykhaylyk, O. O.; Jones, E. R.; Armes, S. P., RAFT Dispersion Alternating Copolymerization of Styrene with N-Phenylmaleimide: Morphology Control and Application as an Aqueous Foam Stabilizer. *Macromolecules* **2016,** *49* (18), 6731-6742.

66. Wang, J.; Wu, Z.; Wang, G.; Matyjaszewski, K., In Situ Crosslinking of Nanoparticles in Polymerization-Induced Self-Assembly via ARGET ATRP of Glycidyl Methacrylate. *Macromol. Rapid Commun.* **2019,** *40* (2), e1800332.

67. Wang, G.; Schmitt, M.; Wang, Z.; Lee, B.; Pan, X.; Fu, L.; Yan, J.; Li, S.; Xie, G.; Bockstaller, M. R.; Matyjaszewski, K., Polymerization-Induced Self-Assembly (PISA) Using ICAR ATRP at Low Catalyst Concentration. *Macromolecules* **2016,** *49* (22), 8605-8615.

68. Wang, K.; Wang, Y.; Zhang, W., Synthesis of diblock copolymer nano-assemblies by PISA under dispersion polymerization: comparison between ATRP and RAFT. *Polym. Chem.* **2017,** *8* (41), 6407-6415.

69. St Thomas, C.; Guerrero-Santos, R.; D'Agosto, F., Alkoxyamine-functionalized latex nanoparticles through RAFT polymerization-induced self-assembly in water. *Polym. Chem.* **2015,** *6* (30), 5405-5413.

70. Darabi, A.; Shirin-Abadi, A. R.; Jessop, P. G.; Cunningham, M. F., Nitroxide-Mediated Polymerization of 2-(Diethylamino)ethyl Methacrylate (DEAEMA) in Water. *Macromolecules* **2015,** *48* (1), 72-80.

71. Darabi, A.; Jessop, P. G.; Cunningham, M. F., One-Pot Synthesis of Poly((diethylamino)ethyl methacrylate-co-styrene)-b-poly(methyl methacrylate-co-styrene) Nanoparticles via Nitroxide-Mediated Polymerization. *Macromolecules* **2015,** *48* (7), 1952-1958.

72. Chiefari, J.; Chong, Y. K.; Ercole, F.; Krstina, J.; Jeffery, J.; Le, T. P. T.; Mayadunne, R. T. A.; Meijs, G. F.; Moad, C. L.; Moad, G.; Rizzardo, E.; Thang, S. H., Living Free-Radical Polymerization by Reversible Addition−Fragmentation Chain Transfer: The RAFT Process. *Macromolecules* **1998,** *31* (16), 5559-5562.

73. Moad, G.; Rizzardo, E.; Thang, S. H., Living Radical Polymerization by the RAFT Process - A Second Update. *Aust. J. Chem.* **2009,** *62* (11), 1402-1472.

74. Moad, G.; Rizzardo, E.; Thang, S. H., Living Radical Polymerization by the RAFT Process - A Third Update. *Aust. J. Chem.* **2012,** *65* (8), 985-1076.

75. Moad, G., RAFT polymerization to form stimuli-responsive polymers. *Polym. Chem.* **2017,** *8* (1), 177-219.

76. Perrier, S., 50th Anniversary Perspective: RAFT Polymerization—A User Guide. *Macromolecules* **2017,** *50* (19), 7433-7447.

77. Hill, M. R.; Carmean, R. N.; Sumerlin, B. S., Expanding the Scope of RAFT Polymerization: Recent Advances and New Horizons. *Macromolecules* **2015,** *48* (16), 5459-5469.

78. McKenzie, T. G.; Fu, Q.; Uchiyama, M.; Satoh, K.; Xu, J.; Boyer, C.; Kamigaito, M.; Qiao, G. G., Beyond Traditional RAFT: Alternative Activation of Thiocarbonylthio Compounds for Controlled Polymerization. *Adv. Sci.* **2016,** *3* (9), 1500394.

79. Corrigan, N.; Yeow, J.; Judzewitsch, P.; Xu, J.; Boyer, C., Seeing the Light: Advancing Materials Chemistry through Photopolymerization. *Angew. Chem. Int. Ed.* **2019,** *58* (16), 5170-5189.

80. Chen, M.; Zhong, M.; Johnson, J. A., Light-Controlled Radical Polymerization: Mechanisms, Methods, and Applications. *Chem. Rev.* **2016,** *116* (17), 10167-10211.

81. Theriot, J. C.; Lim, C.-H.; Yang, H.; Ryan, M. D.; Musgrave, C. B.; Miyake, G. M., Organocatalyzed atom transfer radical polymerization driven by visible light. *Science* **2016,** *352* (6289), 1082-1086.

82. Kottisch, V.; Michaudel, Q.; Fors, B. P., Cationic Polymerization of Vinyl Ethers Controlled by Visible Light. *J. Am. Chem. Soc.* **2016,** *138* (48), 15535-15538.

83. Discekici, E. H.; Anastasaki, A.; Read de Alaniz, J.; Hawker, C. J., Evolution and Future Directions of Metal-Free Atom Transfer Radical Polymerization. *Macromolecules* **2018,** *51* (19), 7421-7434.

84. Wiesbrock, F.; Hoogenboom, R.; Schubert, U. S., Microwave-Assisted Polymer Synthesis: State-of-the-Art and Future Perspectives. *Macromol. Rapid Commun.* **2004,** *25* (20), 1739-1764.

85. An, Z.; Shi, Q.; Tang, W.; Tsung, C.-K.; Hawker, C. J.; Stucky, G. D., Facile RAFT Precipitation Polymerization for the Microwave-Assisted Synthesis of Well-Defined, Double Hydrophilic Block Copolymers and Nanostructured Hydrogels. *J. Am. Chem. Soc.* **2007,** *129* (46), 14493-14499.

86. Garrett, E. T.; Pei, Y.; Lowe, A. B., Microwave-assisted synthesis of block copolymer nanoparticles via RAFT with polymerization-induced self-assembly in methanol. *Polym. Chem.* **2016,** *7* (2), 297-301.

87. Hoogenboom, R.; Schubert, U. S., Microwave-Assisted Polymer Synthesis: Recent Developments in a Rapidly Expanding Field of Research. *Macromol. Rapid Commun.* **2007,** *28* (4), 368-386.

88. Sigg, S. J.; Seidi, F.; Renggli, K.; Silva, T. B.; Kali, G.; Bruns, N., Horseradish Peroxidase as a Catalyst for Atom Transfer Radical Polymerization. *Macromol. Rapid Commun.* **2011,** *32* (21), 1710-1715.

89. Ng, Y.-H.; di Lena, F.; Chai, C. L. L., PolyPEGA with predetermined molecular weights from enzyme-mediated radical polymerization in water. *Chem. Commun.* **2011,** *47* (22), 6464-6466.

90. Zhang, B.; Wang, X.; Zhu, A.; Ma, K.; Lv, Y.; Wang, X.; An, Z., Enzyme-Initiated Reversible Addition–Fragmentation Chain Transfer Polymerization. *Macromolecules* **2015,** *48* (21), 7792-7802.

91. Danielson, A. P.; Van Kuren, D. B.-.; Lucius, M. E.; Makaroff, K.; Williams, C.; Page, R. C.; Berberich, J. A.; Konkolewicz, D., Well-Defined Macromolecules Using Horseradish Peroxidase as a RAFT Initiase. *Macromol. Rapid Commun.* **2016,** *37* (4), 362-367.

92. Enciso, A. E.; Fu, L.; Lathwal, S.; Olszewski, M.; Wang, Z.; Das, S. R.; Russell, A. J.; Matyjaszewski, K., Biocatalytic "Oxygen-Fueled" Atom Transfer Radical Polymerization. *Angew. Chem. Int. Ed.* **2018,** *57* (49), 16157-16161.

93. Chmielarz, P.; Fantin, M.; Park, S.; Isse, A. A.; Gennaro, A.; Magenau, A. J. D.; Sobkowiak, A.; Matyjaszewski, K., Electrochemically mediated atom transfer radical polymerization (eATRP). *Prog. Polym. Sci.* **2017,** *69*, 47-78.

94. Magenau, A. J. D.; Strandwitz, N. C.; Gennaro, A.; Matyjaszewski, K., Electrochemically Mediated Atom Transfer Radical Polymerization. *Science* **2011,** *332* (6025), 81-84.

95. Wang, Y.; Fantin, M.; Park, S.; Gottlieb, E.; Fu, L.; Matyjaszewski, K., Electrochemically Mediated Reversible Addition–Fragmentation Chain-Transfer Polymerization. *Macromolecules* **2017,** *50* (20), 7872-7879.

96. Sang, W.; Xu, M.; Yan, Q., Coenzyme-Catalyzed Electro-RAFT Polymerization. *ACS Macro Lett.* **2017,** *6* (12), 1337-1341.

97. Peterson, B. M.; Lin, S.; Fors, B. P., Electrochemically Controlled Cationic Polymerization of Vinyl Ethers. *J. Am. Chem. Soc.* **2018,** *140* (6), 2076-2079.

98. Mohapatra, H.; Kleiman, M.; Esser-Kahn, A. P., Mechanically controlled radical polymerization initiated by ultrasound. *Nat. Chem.* **2016,** *9*, 135.

99. Wang, Z.; Pan, X.; Yan, J.; Dadashi-Silab, S.; Xie, G.; Zhang, J.; Wang, Z.; Xia, H.; Matyjaszewski, K., Temporal Control in Mechanically Controlled Atom Transfer Radical Polymerization Using Low ppm of Cu Catalyst. *ACS Macro Lett.* **2017,** *6* (5), 546-549.

100. Wang, Z.; Pan, X.; Li, L.; Fantin, M.; Yan, J.; Wang, Z.; Wang, Z.; Xia, H.; Matyjaszewski, K., Enhancing Mechanically Induced ATRP by Promoting Interfacial Electron Transfer from Piezoelectric Nanoparticles to Cu Catalysts. *Macromolecules* **2017,** *50* (20), 7940-7948.

101. McKenzie, T. G.; Colombo, E.; Fu, Q.; Ashokkumar, M.; Qiao, G. G., Sono-RAFT Polymerization in Aqueous Medium. *Angew. Chem. Int. Ed.* **2017,** *56* (40), 12302-12306.

102. Esser, P.; Pohlmann, B.; Scharf, H.-D., The Photochemical Synthesis of Fine Chemicals with Sunlight. *Angew. Chem. Int. Ed.* **1994,** *33* (20), 2009-2023.

103. Oelckers, S.; Hanke, T.; Röder, B., Quenching of singlet oxygen in dimethylformamide. *Journal of Photochemistry and Photobiology A: Chemistry* **2000,** *132* (1), 29-32.

104. Burridge, K. M.; Wright, T. A.; Page, R. C.; Konkolewicz, D., Photochemistry for Well-Defined Polymers in Aqueous Media: From Fundamentals to Polymer Nanoparticles to Bioconjugates. *Macromol. Rapid Commun.* **2018,** *39* (12), 1800093.

105. Yeow, J.; Xu, J.; Boyer, C., Polymerization-Induced Self-Assembly Using Visible Light Mediated Photoinduced Electron Transfer–Reversible Addition–Fragmentation Chain Transfer Polymerization. *ACS Macro Lett.* **2015,** *4* (9), 984-990.

106. Yeow, J.; Sugita, O. R.; Boyer, C., Visible Light-Mediated Polymerization-Induced Self-Assembly in the Absence of External Catalyst or Initiator. *ACS Macro Lett.* **2016,** *5* (5), 558-564.

107. Tan, J.; Sun, H.; Yu, M.; Sumerlin, B. S.; Zhang, L., Photo-PISA: Shedding Light on Polymerization-Induced Self-Assembly. *ACS Macro Lett.* **2015,** *4* (11), 1249-1253.

108. Albertsen, A. N.; Szymański, J. K.; Pérez-Mercader, J., Emergent Properties of Giant Vesicles Formed by a Polymerization-Induced Self-Assembly (PISA) Reaction. *Scientific Reports* **2017,** *7*, 41534.

109. Cheng, G.; Perez-Mercader, J., Polymerization-Induced Self-Assembly for Artificial Biology: Opportunities and Challenges. *Macromol. Rapid Commun.* **2019,** *40* (2), e1800513.

110. Ren, K. X.; Perez-Mercader, J., Light-induced evolution of microaggregates: transformation to vesicles, cyclic growth and collapse and vesicle fusion. *Polym. Chem.* **2018,** *9* (26), 3594-3599.

111. Liu, G.; Qiu, Q.; Shen, W.; An, Z., Aqueous dispersion polymerization of 2-methoxyethyl acrylate for the synthesis of biocompatible nanoparticles using a hydrophilic RAFT polymer and a redox initiator. *Macromolecules* **2011,** *44* (13), 5237-5245.

112. Tan, J.; Xu, Q.; Li, X.; He, J.; Zhang, Y.; Dai, X.; Yu, L.; Zeng, R.; Zhang, L., Enzyme-PISA: An Efficient Method for Preparing Well-Defined Polymer Nano-Objects under Mild Conditions. *Macromol. Rapid Commun.* **2018,** *39* (9), 1700871.

113. Zhou, F.; Li, R.; Wang, X.; Du, S.; An, Z., Non-natural Photoenzymatic Controlled Radical Polymerization Inspired by DNA Photolyase. *Angew. Chem. Int. Ed.* **2019**, *58* (28), 9479-9484.

114. Zhou, Y.-N.; Li, J.-J.; Ljubic, D.; Luo, Z.-H.; Zhu, S., Mechanically Mediated Atom Transfer Radical Polymerization: Exploring Its Potential at High Conversions. *Macromolecules* **2018,** *51* (17), 6911-6921.

115. Wang, Z.; Wang, Z.; Pan, X.; Fu, L.; Lathwal, S.; Olszewski, M.; Yan, J.; Enciso, A. E.; Wang, Z.; Xia, H.; Matyjaszewski, K., Ultrasonication-Induced Aqueous Atom Transfer Radical Polymerization. *ACS Macro Lett.* **2018,** *7* (3), 275-280.

116. Collins, J.; McKenzie, T. G.; Nothling, M. D.; Allison-Logan, S.; Ashokkumar, M.; Qiao, G. G., Sonochemically Initiated RAFT Polymerization in Organic Solvents. *Macromolecules* **2019,** *52* (1), 185-195.

117. McKenzie, T. G.; Reyhani, A.; Nothling, M. D.; Qiao, G. G., Hydroxyl Radical Activated RAFT Polymerization. In *Reversible Deactivation Radical Polymerization: Mechanisms and Synthetic Methodologies*, American Chemical Society: 2018; Vol. 1284, pp 307-321.

118. Pioge, S.; Tran, T. N.; McKenzie, T. G.; Pascual, S.; Ashokkumar, M.; Fontaine, L.; Qiao, G., Sono-RAFT Polymerization-Induced Self-Assembly in Aqueous Dispersion: Synthesis of LCST-type Thermosensitive Nanogels. *Macromolecules* **2018,** *51* (21), 8862-8869.

119. Touve, M. A.; Figg, C. A.; Wright, D. B.; Park, C.; Cantlon, J.; Sumerlin, B. S.; Gianneschi, N. C., Polymerization-Induced Self-Assembly of Micelles Observed by Liquid Cell Transmission Electron Microscopy. *ACS Central Sci.* **2018,** *4* (5), 543-547.

120. Kim, K. H.; Kim, J.; Jo, W. H., Preparation of hydrogel nanoparticles by atom transfer radical polymerization of N-isopropylacrylamide in aqueous media using PEG macro-initiator. *Polymer* **2005,** *46* (9), 2836-2840.

121. Liu, X.; Gao, W., In Situ Growth of Self-Assembled Protein–Polymer Nanovesicles for Enhanced Intracellular Protein Delivery. *ACS Appl. Mat. Inter.* **2017,** *9* (3), 2023-2028.

122. Groison, E.; Brusseau, S.; D'Agosto, F.; Magnet, S.; Inoubli, R.; Couvreur, L.; Charleux, B., Well-Defined Amphiphilic Block Copolymer Nanoobjects via Nitroxide-Mediated Emulsion Polymerization. *ACS Macro Lett.* **2012,** *1* (1), 47-51.

123. Qiao, X. G.; Lansalot, M.; Bourgeat-Lami, E.; Charleux, B., Nitroxide-Mediated Polymerization-Induced Self-Assembly of Poly(poly(ethylene oxide) methyl ether methacrylate-co-styrene)-b-poly(n-butyl methacrylate-co-styrene) Amphiphilic Block Copolymers. *Macromolecules* **2013,** *46* (11), 4285-4295.

124. Delaittre, G.; Dire, C.; Rieger, J.; Putaux, J. L.; Charleux, B., Formation of polymer vesicles by simultaneous chain growth and self-assembly of amphiphilic block copolymers. *Chem. Commun.* **2009,** (20), 2887-2889.

125. Qiao, X. G.; Dugas, P. Y.; Charleux, B.; Lansalot, M.; Bourgeat-Lami, E., Nitroxide-mediated polymerization-induced self-assembly of amphiphilic block copolymers with a pH/temperature dual sensitive stabilizer block. *Polym. Chem.* **2017,** *8* (27), 4014-4029.

126. Sarkar, J.; Xiao, L.; Jackson, A. W.; van Herk, A. M.; Goto, A., Synthesis of transition-metal-free and sulfur-free nanoparticles and nanocapsules via reversible complexation mediated polymerization (RCMP) and polymerization induced self-assembly (PISA). *Polym. Chem.* **2018,** *9* (39), 4900-4907.

127. Shanmugam, S.; Xu, J.; Boyer, C., Exploiting Metalloporphyrins for Selective Living Radical Polymerization Tunable over Visible Wavelengths. *J. Am. Chem. Soc.* **2015,** *137* (28), 9174-9185.

128. Zhou, D.; Kuchel, R. P.; Zetterlund, P. B., A new paradigm in polymerization induced self-assembly (PISA): Exploitation of “non-living” addition–fragmentation chain transfer (AFCT) polymerization. *Polym. Chem.* **2017,** *8* (29), 4177-4181.

129. Lotierzo, A.; Schofield, R. M.; Bon, S. A. F., Toward Sulfur-Free RAFT Polymerization Induced Self-Assembly. *ACS Macro Lett.* **2017,** *6* (12), 1438-1443.

130. Tanaka, H.; Yamauchi, K.; Hasegawa, H.; Miyamoto, N.; Koizumi, S.; Hashimoto, T., In situ and real-time small-angle neutron scattering studies of living anionic polymerization process and polymerization-induced self-assembly of block copolymers. *Phys. B: Condensed Matter* **2006,** *385-386*, 742-744.

131. Boott, C. E.; Gwyther, J.; Harniman, R. L.; Hayward, D. W.; Manners, I., Scalable and uniform 1D nanoparticles by synchronous polymerization, crystallization and self-assembly. *Nat. Chem.* **2017,** *9*, 785.

132. Zhang, L.; Song, C.; Yu, J.; Yang, D.; Xie, M., One-pot synthesis of polymeric nanoparticle by ring-opening metathesis polymerization. *J. Polym. Sci., Part A: Polym. Chem.* **2010,** *48* (22), 5231-5238.

133. Wright, D. B.; Touve, M. A.; Adamiak, L.; Gianneschi, N. C., ROMPISA: Ring-Opening Metathesis Polymerization-Induced Self-Assembly. *ACS Macro Lett.* **2017,** *6* (9), 925-929.

134. Foster, J. C.; Varlas, S.; Blackman, L. D.; Arkinstall, L. A.; O'Reilly, R. K., Ring-Opening Metathesis Polymerization in Aqueous Media Using a Macroinitiator Approach. *Angew. Chem. Int. Ed.* **2018,** *57* (33), 10672-10676.

135. Yu, Q.; Ding, Y.; Cao, H.; Lu, X.; Cai, Y., Use of Polyion Complexation for Polymerization-Induced Self-Assembly in Water under Visible Light Irradiation at 25 °C. *ACS Macro Lett.* **2015,** *4* (11), 1293-1296.

136. Ding, Y.; Cai, M.; Cui, Z.; Huang, L.; Wang, L.; Lu, X.; Cai, Y., Synthesis of Low-Dimensional Polyion Complex Nanomaterials via Polymerization-Induced Electrostatic Self-Assembly. *Angew. Chem. Int. Ed.* **2018,** *57* (4), 1053-1056.

137. Cai, M.; Ding, Y.; Wang, L.; Huang, L.; Lu, X.; Cai, Y., Synthesis of One-Component Nanostructured Polyion Complexes via Polymerization-Induced Electrostatic Self-Assembly. *ACS Macro Lett.* **2018,** *7* (2), 208-212.

138. Wang, L.; Ding, Y.; Liu, Q.; Zhao, Q.; Dai, X.; Lu, X.; Cai, Y., Sequence-Controlled Polymerization-Induced Self-Assembly. *ACS Macro Lett.* **2019,** *8* (5), 623-628.

139. Howe, D. H.; Hart, J. L.; McDaniel, R. M.; Taheri, M. L.; Magenau, A. J. D., Functionalization-Induced Self-Assembly of Block Copolymers for Nanoparticle Synthesis. *ACS Macro Lett.* **2018,** *7* (12), 1503-1508.

140. Chen, L.; Xu, M.; Hu, J.; Yan, Q., Light-Initiated in Situ Self-Assembly (LISA) from Multiple Homopolymers. *Macromolecules* **2017,** *50* (11), 4276-4280.

141. Penfold, N. J. W.; Lovett, J. R.; Verstraete, P.; Smets, J.; Armes, S. P., Stimulus-responsive non-ionic diblock copolymers: protonation of a tertiary amine end-group induces vesicle-to-worm or vesicle-to-sphere transitions. *Polym. Chem.* **2017,** *8*, 272-282.

142. Penfold, N. J. W.; Lovett, J. R.; Warren, N. J.; Verstraete, P.; Smets, J.; Armes, S. P., pH-responsive non-ionic diblock copolymers: protonation of a morpholine end-group induces an order-order transition. *Polym. Chem.* **2016,** *7*, 79-88.

143. Lovett, J. R.; Warren, N. J.; Armes, S. P.; Smallridge, M. J.; Cracknell, R. B., Order-Order Morphological Transitions for Dual Stimulus Responsive Diblock Copolymer Vesicles. *Macromolecules* **2016,** *49* (3), 1016-1025.

144. Lovett, J. R.; Warren, N. J.; Ratcliffe, L. P. D.; Kocik, M. K.; Armes, S. P., pH-responsive non-ionic diblock copolymers: Ionization of carboxylic acid end-groups induces an order–order morphological transition. *Angew. Chem. Int. Ed.* **2015,** *54* (4), 1279-1283.

145. Yao, H.; Ning, Y.; Jesson, C. P.; He, J.; Deng, R.; Tian, W.; Armes, S. P., Using Host-Guest Chemistry to Tune the Kinetics of Morphological Transitions Undertaken by Block Copolymer Vesicles. *ACS Macro Lett.* **2017,** *6* (12), 1379-1385.

146. Xu, S.; Yeow, J.; Boyer, C., Exploiting Wavelength Orthogonality for Successive Photoinduced Polymerization-Induced Self-Assembly and Photo-Crosslinking. *ACS Macro Lett.* **2018,** *7* (11), 1376-1382.

147. Sobotta, F. H.; Hausig, F.; Harz, D. O.; Hoeppener, S.; Schubert, U. S.; Brendel, J. C., Oxidation-responsive micelles by a one-pot polymerization-induced self-assembly approach. *Polym. Chem.* **2018,** *9* (13), 1593-1602.

148. Truong, N. P.; Dussert, M. V.; Whittaker, M. R.; Quinn, J. F.; Davis, T. P., Rapid synthesis of ultrahigh molecular weight and low polydispersity polystyrene diblock copolymers by RAFT-mediated emulsion polymerization. *Polym. Chem.* **2015,** *6* (20), 3865-3874.

149. Cockram, A. A.; Neal, T. J.; Derry, M. J.; Mykhaylyk, O. O.; Williams, N. S. J.; Murray, M. W.; Emmett, S. N.; Armes, S. P., Effect of Monomer Solubility on the Evolution of Copolymer Morphology during Polymerization-Induced Self-Assembly in Aqueous Solution. *Macromolecules* **2017,** *50* (3), 796-802.

150. Waits, C. M.; Ghodssi, R.; Ervin, M. H.; Dubey, M. In *MEMS-based gray-scale lithography*, 2001 International Semiconductor Device Research Symposium. Symposium Proceedings (Cat. No.01EX497), 5-7 Dec. 2001; 2001; pp 182-185.

151. Canton, I.; Warren, N. J.; Chahal, A.; Amps, K.; Wood, A.; Weightman, R.; Wang, E.; Moore, H.; Armes, S. P., Mucin-Inspired Thermoresponsive Synthetic Hydrogels Induce Stasis in Human Pluripotent Stem Cells and Human Embryos. *ACS Central Sci.* **2016,** *2* (2), 65-74.

152. Mitchell, D. E.; Lovett, J. R.; Armes, S. P.; Gibson, M. I., Combining biomimetic block copolymer worms with an ice-inhibiting polymer for the solvent-free cryopreservation of red blood cells. *Angew. Chem. Int. Ed.* **2016,** *55* (8), 2801-2804.

153. Lovett, J. R.; Derry, M. J.; Yang, P.; Hatton, F. L.; Warren, N. J.; Fowler, P. W.; Armes, S. P., Can percolation theory explain the gelation behavior of diblock copolymer worms? *Chem. Sci.* **2018,** *9* (35), 7138-7144.

154. Cates, M. E., Reptation of living polymers: dynamics of entangled polymers in the presence of reversible chain-scission reactions. *Macromolecules* **1987,** *20* (9), 2289-96.

155. Dreiss, C. A., Wormlike micelles: where do we stand? Recent developments, linear rheology and scattering techniques. *Soft Matt.* **2007,** *3* (8), 956-970.

156. Pei, Y.; Jarrett, K.; Saunders, M.; Roth, P. J.; Buckley, C. E.; Lowe, A. B., Triply responsive soft matter nanoparticles based on poly[oligo(ethylene glycol) methyl ether methacrylate-block-3-phenylpropyl methacrylate] copolymers. *Polym. Chem.* **2016,** *7* (15), 2740-2750.

157. Pei, Y.; Sugita, O. R.; Thurairajah, L.; Lowe, A. B., Synthesis of poly(stearyl methacrylate-b-3-phenylpropyl methacrylate) nanoparticles in n-octane and associated thermoreversible polymorphism. *RSC Adv.* **2015,** *5* (23), 17636-17646.

158. Warren, N. J.; Derry, M. J.; Mykhaylyk, O. O.; Lovett, J. R.; Ratcliffe, L. P. D.; Ladmiral, V.; Blanazs, A.; Fielding, L. A.; Armes, S. P., Critical Dependence of Molecular Weight on Thermoresponsive Behavior of Diblock Copolymer Worm Gels in Aqueous Solution. *Macromolecules* **2018,** *51* (21), 8357-8371.

159. Tan, J.; Bai, Y.; Zhang, X.; Zhang, L., Room temperature synthesis of poly(poly(ethylene glycol) methyl ether methacrylate)-based diblock copolymer nano-objects via Photoinitiated Polymerization-Induced Self-Assembly (Photo-PISA). *Polym. Chem.* **2016,** *7* (13), 2372-2380.

160. Doncom, K. E. B.; Warren, N. J.; Armes, S. P., Polysulfobetaine-based diblock copolymer nano-objects via polymerization-induced self-assembly. *Polym. Chem.* **2015,** *6*, 7264-7273.

161. Ren, K.; Perez-Mercader, J., Thermoresponsive gels directly obtained via visible light-mediated polymerization-induced self-assembly with oxygen tolerance. *Polym. Chem.* **2017,** *8* (23), 3548-3552.

162. Figg, C. A.; Carmean, R. N.; Bentz, K. C.; Mukherjee, S.; Savin, D. A.; Sumerlin, B. S., Tuning Hydrophobicity To Program Block Copolymer Assemblies from the Inside Out. *Macromolecules* **2017,** *50* (3), 935-943.

163. Wang, X.; Figg, C. A.; Lv, X.; Yang, Y.; Sumerlin, B. S.; An, Z., Star Architecture Promoting Morphological Transitions during Polymerization-Induced Self-Assembly. *ACS Macro Lett.* **2017,** *6* (4), 337-342.

164. Gao, P.; Cao, H.; Ding, Y.; Cai, M.; Cui, Z.; Lu, X.; Cai, Y., Synthesis of Hydrogen-Bonded Pore-Switchable Cylindrical Vesicles via Visible-Light-Mediated RAFT Room-Temperature Aqueous Dispersion Polymerization. *ACS Macro Lett.* **2016,** *5* (12), 1327-1331.

165. Ma, Y. J.; Gao, P.; Ding, Y.; Huang, L. L.; Wang, L.; Lu, X. H.; Cai, Y. L., Visible Light Initiated Thermoresponsive Aqueous Dispersion Polymerization-Induced Self-Assembly. *Macromolecules* **2019**, *52* (3), 1033-1041.

166. Zhou, W.; Qu, Q.; Xu, Y.; An, Z., Aqueous Polymerization-Induced Self-Assembly for the Synthesis of Ketone-Functionalized Nano-Objects with Low Polydispersity. *ACS Macro Lett.* **2015,** *4* (5), 495-499.

167. Qu, Q.; Liu, G.; Lv, X.; Zhang, B.; An, Z., In Situ Cross-Linking of Vesicles in Polymerization-Induced Self-Assembly. *ACS Macro Lett.* **2016,** *5* (3), 316-320.

168. Ratcliffe, L. P. D.; McKenzie, B. E.; Le Bouedec, G. M. D.; Williams, C. N.; Brown, S. L.; Armes, S. P., Polymerization-Induced Self-Assembly of All-Acrylic Diblock Copolymers via RAFT Dispersion Polymerization in Alkanes. *Macromolecules* **2015,** *48* (23), 8594-8607.

169. Tan, J.; Li, X.; Zeng, R.; Liu, D.; Xu, Q.; He, J.; Zhang, Y.; Dai, X.; Yu, L.; Zeng, Z.; Zhang, L., Expanding the Scope of Polymerization-Induced Self-Assembly: Z-RAFT-Mediated Photoinitiated Dispersion Polymerization. *ACS Macro Lett.* **2018,** *7* (2), 255-262.

170. Perrier, S.; Takolpuckdee, P.; Mars, C. A., Reversible Addition−Fragmentation Chain Transfer Polymerization Mediated by a Solid Supported Chain Transfer Agent. *Macromolecules* **2005,** *38* (16), 6770-6774.

171. Zhao; Perrier, S., Synthesis of Well-Defined Homopolymer and Diblock Copolymer Grafted onto Silica Particles by Z-Supported RAFT Polymerization. *Macromolecules* **2006,** *39* (25), 8603-8608.

172. Canning, S. L.; Cunningham, V. J.; Ratcliffe, L. P. D.; Armes, S. P., Phenyl acrylate is a versatile monomer for the synthesis of acrylic diblock copolymer nano-objects via polymerization-induced self-assembly. *Polym. Chem.* **2017,** *8* (33), 4811-4821.

173. Derry, M. J.; Mykhaylyk, O. O.; Armes, S. P., A Vesicle-to-Worm Transition Provides a New High-Temperature Oil Thickening Mechanism. *Angew. Chem. Int. Ed.* **2017,** *56* (7), 1746-1750.

174. Gibson, R. R.; Armes, S. P.; Musa, O. M.; Fernyhough, A., End-group ionisation enables the use of poly(N-(2-methacryloyloxy)ethyl pyrrolidone) as an electrosteric stabiliser block for polymerisation-induced self-assembly in aqueous media. *Polym. Chem.* **2019,** *10* (11), 1312-1323.

175. Bütün, V.; Armes, S. P.; Billingham, N. C., Synthesis and aqueous solution properties of near-monodisperse tertiary amine methacrylate homopolymers and diblock copolymers. *Polymer* **2001,** *42* (14), 5993-6008.

176. Canning, S. L.; Neal, T. J.; Armes, S. P., pH-Responsive Schizophrenic Diblock Copolymers Prepared by Polymerization-Induced Self-Assembly. *Macromolecules* **2017,** *50* (16), 6108-6116.

177. Bütün, V.; Liu, S.; Weaver, J. V. M.; Bories-Azeau, X.; Cai, Y.; Armes, S. P., A brief review of 'schizophrenic' block copolymers. *React. Funct. Polym.* **2006,** *66* (1), 157-165.

178. Tan, J.; Zhang, X.; Liu, D.; Bai, Y.; Huang, C.; Li, X.; Zhang, L., Facile Preparation of CO2-Responsive Polymer Nano-Objects via Aqueous Photoinitiated Polymerization-Induced Self-Assembly (Photo-PISA). *Macromol. Rapid Commun.* **2017,** *38* (13), 1600508.

179. Morse, A. J.; Armes, S. P.; Thompson, K. L.; Dupin, D.; Fielding, L. A.; Mills, P.; Swart, R., Novel Pickering emulsifiers based on pH-responsive poly(2-(diethylamino)ethyl methacrylate) latexes. *Langmuir* **2013,** *29* (18), 5466-75.

180. Babin, J.; Pelletier, M.; Lepage, M.; Allard, J.-F.; Morris, D.; Zhao, Y., A New Two-Photon-Sensitive Block Copolymer Nanocarrier. *Angew. Chem. Int. Ed.* **2009,** *48* (18), 3329-3332.

181. Jiang, Y.; Hu, X.; Hu, J.; Liu, H.; Zhong, H.; Liu, S., Reactive Fluorescence Turn-On Probes for Fluoride Ions in Purely Aqueous Media Fabricated from Functionalized Responsive Block Copolymers. *Macromolecules* **2011,** *44* (22), 8780-8790.

182. Jin, Q.; Liu, G.; Ji, J., Micelles and reverse micelles with a photo and thermo double-responsive block copolymer. *J. Polym. Sci., Part A: Polym. Chem.* **2010,** *48* (13), 2855-2861.

183. Jiang, J.; Qi, B.; Lepage, M.; Zhao, Y., Polymer Micelles Stabilization on Demand through Reversible Photo-Cross-Linking. *Macromolecules* **2007,** *40* (4), 790-792.

184. Jin, Q.; Liu, G.; Ji, J., Preparation of reversibly photo-cross-linked nanogels from pH-responsive block copolymers and use as nanoreactors for the synthesis of gold nanoparticles. *Eur. Polym. J.* **2010,** *46* (11), 2120-2128.

185. Zhang, W.-J.; Hong, C.-Y.; Pan, C.-Y., Artificially Smart Vesicles with Superior Structural Stability: Fabrication, Characterizations, and Transmembrane Traffic. *ACS Appl. Mat. Inter.* **2017,** *9* (17), 15086-15095.

186. Chen, M.; Li, J. W.; Zhang, W. J.; Hong, C. Y.; Pan, C. Y., pH- and Reductant-Responsive Polymeric Vesicles with Robust Membrane-Cross-Linked Structures: In Situ Cross-Linking in Polymerization-Induced Self-Assembly. *Macromolecules* **2019,** *52* (3), 1140-1149.

187. O'Reilly, R. K.; Hawker, C. J.; Wooley, K. L., Crosslinked block copolymer micelles: functional nanostructures of great potential and versatility. *Chem. Soc. Rev.* **2006,** *35* (11), 1068-1083.

188. Read, E. S.; Armes, S. P., Recent advances in shell cross-linked micelles. *Chem. Commun.* **2007,** (29), 3021-3035.

189. Thurmond, K. B.; Kowalewski, T.; Wooley, K. L., Water-Soluble Knedel-like Structures: The Preparation of Shell-Cross-Linked Small Particles. *J. Am. Chem. Soc.* **1996,** *118* (30), 7239-7240.

190. Zhang, W.-J.; Hong, C.-Y.; Pan, C.-Y., Polymerization-Induced Self-Assembly of Functionalized Block Copolymer Nanoparticles and Their Application in Drug Delivery. *Macromol. Rapid Commun.* **2019,** *40* (2), e1800279.

191. Sugihara, S.; Armes, S. P.; Blanazs, A.; Lewis, A. L., Non-spherical morphologies from cross-linked biomimetic diblock copolymers using RAFT aqueous dispersion polymerization. *Soft Matt.* **2011,** *7* (22), 10787-10793.

192. Thompson, K. L.; Mable, C. J.; Cockram, A.; Warren, N. J.; Cunningham, V. J.; Jones, E. R.; Verber, R.; Armes, S. P., Are block copolymer worms more effective Pickering emulsifiers than block copolymer spheres? *Soft Matt.* **2014,** *10* (43), 8615-8626.

193. Thompson, K. L.; Chambon, P.; Verber, R.; Armes, S. P., Can Polymersomes Form Colloidosomes? *J. Am. Chem. Soc.* **2012,** *134* (30), 12450-12453.

194. Chambon, P.; Blanazs, A.; Battaglia, G.; Armes, S. P., How does cross-linking affect the stability of block copolymer vesicles in the presence of surfactant? *Langmuir* **2012,** *28* (2), 1196-1205.

195. Hatton, F. L.; Lovett, J. R.; Armes, S. P., Synthesis of well-defined epoxy-functional spherical nanoparticles by RAFT aqueous emulsion polymerization. *Polym. Chem.* **2017,** *8* (33), 4856-4868.

196. Hunter, S. J.; Thompson, K. L.; Lovett, J. R.; Hatton, F. L.; Derry, M. J.; Lindsay, C.; Taylor, P.; Armes, S. P., Synthesis, Characterization, and Pickering Emulsifier Performance of Anisotropic Cross-Linked Block Copolymer Worms: Effect of Aspect Ratio on Emulsion Stability in the Presence of Surfactant. *Langmuir* **2019,** *35* (1), 254-265.

197. Lovett, J. R.; Ratcliffe, L. P. D.; Warren, N. J.; Armes, S. P.; Saunders, B. R., A robust cross-linking strategy for block copolymer worms prepared via polymerization-induced self-assembly. *Macromolecules* **2016,** *49* (8), 2928-2941.

198. Penfold, N. J. W.; Ning, Y.; Verstraete, P.; Smets, J.; Armes, S. P., Cross-Linked Cationic Diblock Copolymer Worms are Superflocculants for Micrometer-sized Silica Particles. *Chem. Sci.* **2016,** *7* (12), 6894-6904.

199. Penfold, N. J. W.; Parnell, A. J.; Molina, M.; Verstraete, P.; Smets, J.; Armes, S. P., Layer-By-Layer Self-Assembly of Polyelectrolytic Block Copolymer Worms on a Planar Substrate. *Langmuir* **2017,** *33* (50), 14425-14436.

200. Tan, J.; Liu, D.; Huang, C.; Li, X.; He, J.; Xu, Q.; Zhang, L., Photoinitiated Polymerization-Induced Self-Assembly of Glycidyl Methacrylate for the Synthesis of Epoxy-Functionalized Block Copolymer Nano-Objects. *Macromol. Rapid Commun.* **2017,** *38* (15), n/a.

201. Ratcliffe, L. P. D.; Ryan, A. J.; Armes, S. P., From a Water-Immiscible Monomer to Block Copolymer Nano-Objects via a One-Pot RAFT Aqueous Dispersion Polymerization Formulation. *Macromolecules* **2013,** *46* (3), 769-777.

202. Tan, J.; Dai, X.; Zhang, Y.; Yu, L.; Sun, H.; Zhang, L., Photoinitiated Polymerization-Induced Self-Assembly via Visible Light-Induced RAFT-Mediated Emulsion Polymerization. *ACS Macro Lett.* **2019,** *8* (2), 205-212.

203. Zhang, X.; Boisse, S.; Zhang, W.; Beaunier, P.; D'Agosto, F.; Rieger, J.; Charleux, B., Well-defined amphiphilic block copolymers and nano-objects formed in situ via raft-mediated aqueous emulsion polymerization. *Macromolecules* **2011,** *44* (11), 4149-4158.

204. Boisse, S.; Rieger, J.; Pembouong, G.; Beaunier, P.; Charleux, B., Influence of the stirring speed and CaCl2 concentration on the nano-object morphologies obtained via RAFT-mediated aqueous emulsion polymerization in the presence of a water-soluble macroRAFT agent. *J. Polym. Sci., Part A: Polym. Chem.* **2011,** *49* (15), 3346-3354.

205. Truong, N. P.; Quinn, J. F.; Anastasaki, A.; Haddleton, D. M.; Whittaker, M. R.; Davis, T. P., Facile access to thermoresponsive filomicelles with tuneable cores. *Chem. Commun.* **2016,** *52* (24), 4497-4500.

206. Khor, S. Y.; Truong, N. P.; Quinn, J. F.; Whittaker, M. R.; Davis, T. P., Polymerization-Induced Self-Assembly: The Effect of End Group and Initiator Concentration on Morphology of Nanoparticles Prepared via RAFT Aqueous Emulsion Polymerization. *ACS Macro Lett.* **2017,** *6* (9), 1013-1019.

207. Docherty, P. J.; Derry, M. J.; Armes, S. P., RAFT dispersion polymerization of glycidyl methacrylate for the synthesis of epoxy-functional block copolymer nanoparticles in mineral oil. *Polym. Chem.* **2019,** *10* (5), 603-611.

208. He, J.; Xu, Q.; Tan, J.; Zhang, L.; Tan, J.; Zhang, L., Ketone-Functionalized Polymer Nano-Objects Prepared via Photoinitiated Polymerization-Induced Self-Assembly (Photo-PISA) Using a Poly(diacetone acrylamide)-Based Macro-RAFT Agent. *Macromol. Rapid Commun.* **2019,** *40* (2), e1800296.

209. Zhang, W.-J.; Hong, C.-Y.; Pan, C.-Y., Efficient Fabrication of Photosensitive Polymeric Nano-objects via an Ingenious Formulation of RAFT Dispersion Polymerization and Their Application for Drug Delivery. *Biomacromolecules* **2017,** *18* (4), 1210-1217.

210. Huang, J.; Li, D.; Liang, H.; Lu, J., Synthesis of Photocrosslinkable and Amine Containing Multifunctional Nanoparticles via Polymerization-Induced Self-Assembly. *Macromol. Rapid Commun.* **2017,** *38* (15), 1700202.

211. Huang, L.; Ding, Y.; Ma, Y.; Wang, L.; Liu, Q.; Lu, X.; Cai, Y., Colloidal Stable PIC Vesicles and Lamellae Enabled by Wavelength-Orthogonal Disulfide Exchange and Polymerization-Induced Electrostatic Self-Assembly. *Macromolecules* **2019,** *52* (12),4703-4712.

212. Chambon, P.; Blanazs, A.; Battaglia, G.; Armes, S. P., Facile Synthesis of Methacrylic ABC Triblock Copolymer Vesicles by RAFT Aqueous Dispersion Polymerization. *Macromolecules* **2012,** *45* (12), 5081-5090.

213. Zhang, L.; Lu, Q.; Lv, X.; Shen, L.; Zhang, B.; An, Z., In Situ Cross-Linking as a Platform for the Synthesis of Triblock Copolymer Vesicles with Diverse Surface Chemistry and Enhanced Stability via RAFT Dispersion Polymerization. *Macromolecules* **2017,** *50* (5), 2165-2174.

214. Zhang, B. H.; Lv, X. Q.; Zhu, A. Q.; Zheng, J. W.; Yang, Y. Q.; An, Z. S., Morphological Stabilization of Block Copolymer Worms Using Asymmetric Cross-Linkers during Polymerization-Induced Self-Assembly. *Macromolecules* **2018,** *51* (8), 2776-2784.

215. Truong, N. P.; Zhang, C.; Nguyen, T. A. H.; Anastasaki, A.; Schulze, M. W.; Quinn, J. F.; Whittaker, A. K.; Hawker, C. J.; Whittaker, M. R.; Davis, T. P., Overcoming Surfactant-Induced Morphology Instability of Noncrosslinked Diblock Copolymer Nano-Objects Obtained by RAFT Emulsion Polymerization. *ACS Macro Lett.* **2018,** *7* (2), 159-165.

216. Sanchez, C.; Belleville, P.; Popall, M.; Nicole, L., Applications of advanced hybrid organic–inorganic nanomaterials: from laboratory to market. *Chem. Soc. Rev.* **2011,** *40* (2), 696-753.

217. Pyun, J.; Matyjaszewski, K., Synthesis of Nanocomposite Organic/Inorganic Hybrid Materials Using Controlled/“Living” Radical Polymerization. *Chem. Mater.* **2001,** *13* (10), 3436-3448.

218. Zhang, Z.; Zhang, P.; Wang, Y.; Zhang, W., Recent advances in organic–inorganic well-defined hybrid polymers using controlled living radical polymerization techniques. *Polym. Chem.* **2016,** *7* (24), 3950-3976.

219. Förster, S.; Antonietti, M., Amphiphilic Block Copolymers in Structure-Controlled Nanomaterial Hybrids. *Adv. Mater.* **1998,** *10* (3), 195-217.

220. Nguyen, D.; Zondanos, H. S.; Farrugia, J. M.; Serelis, A. K.; Such, C. H.; Hawkett, B. S., Pigment Encapsulation by Emulsion Polymerization Using Macro-RAFT Copolymers. *Langmuir* **2008,** *24* (5), 2140-2150.

221. Perreira, A. C.; Pearson, S.; Kostadinova, D.; Leroux, F.; D'Agosto, F.; Lansalot, M.; Bourgeat-Lami, E.; Prévot, V., Nanocomposite latexes containing layered double hydroxides via RAFT-assisted encapsulating emulsion polymerization. *Polym. Chem.* **2017,** *8* (7), 1233-1243.

222. Mable, C. J.; Gibson, R. R.; Prevost, S.; McKenzie, B. E.; Mykhaylyk, O. O.; Armes, S. P., Loading of Silica Nanoparticles in Block Copolymer Vesicles during Polymerization-Induced Self-Assembly: Encapsulation Efficiency and Thermally Triggered Release. *J. Am. Chem. Soc.* **2015,** *137* (51), 16098-16108.

223. Parvole, J.; Chaduc, I.; Ako, K.; Spalla, O.; Thill, A.; Ravaine, S.; Duguet, E.; Lansalot, M.; Bourgeat-Lami, E., Efficient Synthesis of Snowman- and Dumbbell-like Silica/Polymer Anisotropic Heterodimers through Emulsion Polymerization Using a Surface-Anchored Cationic Initiator. *Macromolecules* **2012,** *45* (17), 7009-7018.

224. Ferguson, C. J.; Hughes, R. J.; Pham, B. T. T.; Hawkett, B. S.; Gilbert, R. G.; Serelis, A. K.; Such, C. H., Effective ab Initio Emulsion Polymerization under RAFT Control. *Macromolecules* **2002,** *35* (25), 9243-9245.

225. Ferguson, C. J.; Hughes, R. J.; Nguyen, D.; Pham, B. T. T.; Gilbert, R. G.; Serelis, A. K.; Such, C. H.; Hawkett, B. S., Ab Initio Emulsion Polymerization by RAFT-Controlled Self-Assembly. *Macromolecules* **2005,** *38* (6), 2191-2204.

226. Nguyen, D.; Pham, B. T. T.; Huynh, V.; Kim, B. J.; Pham, N. T. H.; Bickley, S. A.; Jones, S. K.; Serelis, A.; Davey, T.; Such, C.; Hawkett, B. S., Monodispersed polymer encapsulated superparamagnetic iron oxide nanoparticles for cell labeling. *Polymer* **2016,** *106*, 238-248.

227. Huynh, V. T.; Nguyen, D.; Such, C. H.; Hawkett, B. S., Polymer coating of graphene oxide via reversible addition–fragmentation chain transfer mediated emulsion polymerization. *J. Polym. Sci., Part A: Polym. Chem.* **2015,** *53* (12), 1413-1421.

228. Ali, S. I.; Heuts, J. P. A.; Hawkett, B. S.; van Herk, A. M., Polymer Encapsulated Gibbsite Nanoparticles: Efficient Preparation of Anisotropic Composite Latex Particles by RAFT-Based Starved Feed Emulsion Polymerization. *Langmuir* **2009,** *25* (18), 10523-10533.

229. Qiao, X. G.; Dugas, P. Y.; Charleux, B.; Lansalot, M.; Bourgeat-Lami, E., Synthesis of Multipod-like Silica/Polymer Latex Particles via Nitroxide-Mediated Polymerization-Induced Self-Assembly of Amphiphilic Block Copolymers. *Macromolecules* **2015,** *48* (3), 545-556.

230. Qiao, X. G.; Lambert, O.; Taveau, J. C.; Dugas, P. Y.; Charleux, B.; Lansalot, M.; Bourgeat-Lami, E., Nitroxide-Mediated Polymerization-Induced Self-Assembly of Block Copolymers at the Surface of Silica Particles: Toward New Hybrid Morphologies. *Macromolecules* **2017,** *50* (10), 3796-3806.

231. Deng, R.; Derry, M. J.; Mable, C. J.; Ning, Y.; Armes, S. P., Using Dynamic Covalent Chemistry To Drive Morphological Transitions: Controlled Release of Encapsulated Nanoparticles from Block Copolymer Vesicles. *J. Am. Chem. Soc.* **2017,** *139*, 7616-7623.

232. Pham, B. T. T.; Nguyen, D.; Huynh, V. T.; Pan, E. H.; Shirodkar-Robinson, B.; Carey, M.; Serelis, A. K.; Warr, G. G.; Davey, T.; Such, C. H.; Hawkett, B. S., Aqueous Polymeric Hollow Particles as an Opacifier by Emulsion Polymerization Using Macro-RAFT Amphiphiles. *Langmuir* **2018,** *34* (14), 4255-4263.

233. Bourgeat-Lami, E.; Lansalot, M., Organic/Inorganic Composite Latexes: The Marriage of Emulsion Polymerization and Inorganic Chemistry. In *Hybrid Latex Particles: Preparation with (Mini)emulsion Polymerization*, van Herk, A. M.; Landfester, K., Eds. Springer Berlin Heidelberg: Berlin, Heidelberg, 2010; pp 53-123.

234. Rose, S.; Prevoteau, A.; Elzière, P.; Hourdet, D.; Marcellan, A.; Leibler, L., Nanoparticle solutions as adhesives for gels and biological tissues. *Nature* **2013,** *505*, 382.

235. Bischof, J. C.; He, X., Thermal Stability of Proteins. *Ann. N.Y. Acad. Sci.* **2006,** *1066* (1), 12-33.

236. Pelegri-O'Day, E. M.; Lin, E.-W.; Maynard, H. D., Therapeutic Protein–Polymer Conjugates: Advancing Beyond PEGylation. *J. Am. Chem. Soc.* **2014,** *136* (41), 14323-14332.

237. Sumerlin, B. S., Proteins as Initiators of Controlled Radical Polymerization: Grafting-from via ATRP and RAFT. *ACS Macro Lett.* **2012,** *1* (1), 141-145.

238. Averick, S.; Simakova, A.; Park, S.; Konkolewicz, D.; Magenau, A. J. D.; Mehl, R. A.; Matyjaszewski, K., ATRP under Biologically Relevant Conditions: Grafting from a Protein. *ACS Macro Lett.* **2012,** *1* (1), 6-10.

239. Tucker, B. S.; Coughlin, M. L.; Figg, C. A.; Sumerlin, B. S., Grafting-From Proteins Using Metal-Free PET–RAFT Polymerizations under Mild Visible-Light Irradiation. *ACS Macro Lett.* **2017,** *6* (4), 452-457.

240. Liu, J.; Bulmus, V.; Herlambang, D. L.; Barner-Kowollik, C.; Stenzel, M. H.; Davis, T. P., In Situ Formation of Protein–Polymer Conjugates through Reversible Addition Fragmentation Chain Transfer Polymerization. *Angew. Chem. Int. Ed.* **2007,** *46* (17), 3099-3103.

241. Boyer, C.; Bulmus, V.; Liu, J.; Davis, T. P.; Stenzel, M. H.; Barner-Kowollik, C., Well-Defined Protein−Polymer Conjugates via in Situ RAFT Polymerization. *J. Am. Chem. Soc.* **2007,** *129* (22), 7145-7154.

242. Xu, J.; Jung, K.; Corrigan, N. A.; Boyer, C., Aqueous photoinduced living/controlled polymerization: tailoring for bioconjugation. *Chem. Sci.* **2014,** *5* (9), 3568-3575.

243. Blackman, L. D.; Varlas, S.; Arno, M. C.; Fayter, A.; Gibson, M. I.; O'Reilly, R. K., Permeable Protein-Loaded Polymersome Cascade Nanoreactors by Polymerization-Induced Self-Assembly. *ACS Macro Lett.* **2017,** *6* (11), 1263-1267.

244. Blackman, L. D.; Varlas, S.; Arno, M. C.; Houston, Z. H.; Fletcher, N. L.; Thurecht, K. J.; Hasan, M.; Gibson, M. I.; O'Reilly, R. K., Confinement of Therapeutic Enzymes in Selectively Permeable Polymer Vesicles by Polymerization-Induced Self-Assembly (PISA) Reduces Antibody Binding and Proteolytic Susceptibility. *ACS Central Sci.* **2018,** *4* (6), 718-723.

245. Varlas, S.; Blackman, L. D.; Findlay, H. E.; Reading, E.; Booth, P. J.; Gibson, M. I.; O'Reilly, R. K., Photoinitiated Polymerization-Induced Self-Assembly in the Presence of Surfactants Enables Membrane Protein Incorporation into Vesicles. *Macromolecules* **2018,** *51* (16), 6190-6201.

246. Liu, X.; Sun, M.; Sun, J.; Hu, J.; Wang, Z.; Guo, J.; Gao, W., Polymerization Induced Self-Assembly of a Site-Specific Interferon α-Block Copolymer Conjugate into Micelles with Remarkably Enhanced Pharmacology. *J. Am. Chem. Soc.* **2018,** *140* (33), 10435-10438.

247. Ma, C.; Liu, X.; Wu, G.; Zhou, P.; Zhou, Y.; Wang, L.; Huang, X., Efficient Way to Generate Protein-Based Nanoparticles by in-Situ Photoinitiated Polymerization-Induced Self-Assembly. *ACS Macro Lett.* **2017,** *6* (7), 689-694.

248. Yeow, J.; Chapman, R.; Gormley, A. J.; Boyer, C., Up in the air: oxygen tolerance in controlled/living radical polymerisation. *Chem. Soc. Rev.* **2018,** *47* (12), 4357-4387.

249. Guerrero-Sanchez, C.; Paulus, R. M.; Fijten, M. W. M.; de la Mar, M. J.; Hoogenboom, R.; Schubert, U. S., High-throughput experimentation in synthetic polymer chemistry: From RAFT and anionic polymerizations to process development. *Appl. Surf. Sci.* **2006,** *252* (7), 2555-2561.

250. Guerrero-Sanchez, C.; Keddie, D. J.; Saubern, S.; Chiefari, J., Automated Parallel Freeze–Evacuate–Thaw Degassing Method for Oxygen-Sensitive Reactions: RAFT Polymerization. *ACS Comb. Sci.* **2012,** *14* (7), 389-394.

251. Cockram, A. A.; Bradley, R. D.; Lynch, S. A.; Fleming, P. C. D.; Williams, N. S. J.; Murray, M. W.; Emmett, S. N.; Armes, S. P., Optimization of the high-throughput synthesis of multiblock copolymer nanoparticles in aqueous media via polymerization-induced self-assembly. *Reaction Chemistry & Engineering* **2018,** *3* (5), 645-657.

252. Tan, J.; Liu, D.; Bai, Y.; Huang, C.; Li, X.; He, J.; Xu, Q.; Zhang, L., Enzyme-Assisted Photoinitiated Polymerization-Induced Self-Assembly: An Oxygen-Tolerant Method for Preparing Block Copolymer Nano-Objects in Open Vessels and Multiwell Plates. *Macromolecules* **2017,** *50* (15), 5798-5806.

253. Matyjaszewski, K.; Coca, S.; Gaynor, S. G.; Wei, M.; Woodworth, B. E., Controlled Radical Polymerization in the Presence of Oxygen. *Macromolecules* **1998,** *31* (17), 5967-5969.

254. Chapman, R.; Gormley, A. J.; Herpoldt, K.-L.; Stevens, M. M., Highly Controlled Open Vessel RAFT Polymerizations by Enzyme Degassing. *Macromolecules* **2014,** *47* (24), 8541-8547.

255. Oytun, F.; Kahveci, M. U.; Yagci, Y., Sugar overcomes oxygen inhibition in photoinitiated free radical polymerization. *J. Polym. Sci., Part A: Polym. Chem.* **2013,** *51* (8), 1685-1689.

256. Zhang, T.; Yeow, J.; Boyer, C., A Cocktail of Vitamins for Aqueous RAFT Polymerization in an Open-to-Air Microtiter Plate. *Polym. Chem.* **2019,** DOI: 10.1039/C9PY00898E.

257. Ng, G.; Yeow, J.; Chapman, R.; Isahak, N.; Wolvetang, E.; Cooper-White, J. J.; Boyer, C., Pushing the Limits of High Throughput PET-RAFT Polymerization. *Macromolecules* **2018,** *51* (19), 7600-7607.

258. Chapman, R.; Gormley, A. J.; Stenzel, M. H.; Stevens, M. M., Combinatorial Low-Volume Synthesis of Well-Defined Polymers by Enzyme Degassing. *Angew. Chem. Int. Ed.* **2016,** *55* (14), 4500-4503.

259. Yeow, J.; Shanmugam, S.; Corrigan, N.; Kuchel, R. P.; Xu, J.; Boyer, C., A Polymerization-Induced Self-Assembly Approach to Nanoparticles Loaded with Singlet Oxygen Generators. *Macromolecules* **2016,** *49* (19), 7277-7285.

260. Ng, G.; Yeow, J.; Xu, J.; Boyer, C., Application of oxygen tolerant PET-RAFT to polymerization-induced self-assembly. *Polym. Chem.* **2017,** *8* (18), 2841-2851.

261. Yeow, J.; Chapman, R.; Xu, J.; Boyer, C., Oxygen tolerant photopolymerization for ultralow volumes. *Polym. Chem.* **2017,** *8* (34), 5012-5022.

262. Touve, M. A.; Wright, D. B.; Mu, C.; Sun, H.; Park, C.; Gianneschi, N. C., Block Copolymer Amphiphile Phase Diagrams by High-Throughput Transmission Electron Microscopy. *Macromolecules* **2019,** DOI: 10.1021/acs.macromol.9b00563.

263. Plutschack, M. B.; Pieber, B.; Gilmore, K.; Seeberger, P. H., The Hitchhiker's Guide to Flow Chemistry. *Chem. Rev.* **2017,** *117* (18), 11796-11893.

264. Tonhauser, C.; Natalello, A.; Löwe, H.; Frey, H., Microflow Technology in Polymer Synthesis. *Macromolecules* **2012,** *45* (24), 9551-9570.

265. Webb, D.; Jamison, T. F., Continuous flow multi-step organic synthesis. *Chem. Sci.* **2010,** *1* (6), 675-680.

266. Jas, G.; Kirschning, A., Continuous Flow Techniques in Organic Synthesis. *Chem. A Eur. J.* **2003,** *9* (23), 5708-5723.

267. Peng, J.; Tian, C.; Zhang, L.; Cheng, Z.; Zhu, X., The in situ formation of nanoparticles via RAFT polymerization-induced self-assembly in a continuous tubular reactor. *Polym. Chem.* **2017,** *8* (9), 1495-1506.

268. Zaquen, N.; Yeow, J.; Junkers, T.; Boyer, C.; Zetterlund, P. B., Visible Light-Mediated Polymerization-Induced Self-Assembly Using Continuous Flow Reactors. *Macromolecules* **2018,** *51* (14), 5165-5172.

269. Parkinson, S.; Hondow, N. S.; Conteh, J. S.; Bourne, R. A.; Warren, N. J., All-aqueous continuous-flow RAFT dispersion polymerisation for efficient preparation of diblock copolymer spheres, worms and vesicles. *React. Chem. Eng.* **2019,** *4* (5), 852-861.

270. Zaquen, N.; Kadir, A. M. N. B. P. H. A.; Iasa, A.; Corrigan, N.; Junkers, T.; Zetterlund, P. B.; Boyer, C., Rapid Oxygen Tolerant Aqueous RAFT Photopolymerization in Continuous Flow Reactors. *Macromolecules* **2019,** *52* (4), 1609-1619.

271. Zaquen, N.; Zu, H.; Kadir, A. M. N. B. P. H. A.; Junkers, T.; Zetterlund, P. B.; Boyer, C., Scalable Aqueous Reversible Addition–Fragmentation Chain Transfer Photopolymerization-Induced Self-Assembly of Acrylamides for Direct Synthesis of Polymer Nanoparticles for Potential Drug Delivery Applications. *ACS Appl. Polym. Mat.* **2019,** *1* (6), 1251-1256.

272. Junkers, T.; Wenn, B., Continuous photoflow synthesis of precision polymers. *React. Chem. Eng.* **2016,** *1* (1), 60-64.

273. Ding, Y.; Zhao, Q.; Wang, L.; Huang, L.; Liu, Q.; Lu, X.; Cai, Y., Polymerization-Induced Self-Assembly Promoted by Liquid–Liquid Phase Separation. *ACS Macro Lett.* **2019**, 943-946.

274. Varlas, S.; Foster, J. C.; Arkinstall, L. A.; Jones, J. R.; Keogh, R.; Mathers, R. T.; O'Reilly, R. K., Predicting Monomers for Use in Aqueous Ring-Opening Metathesis Polymerization-Induced Self-Assembly. *ACS Macro Lett.* **2019,** *8* (4), 466-472.

275. Foster, J. C.; Varlas, S.; Couturaud, B.; Jones, J. R.; Keogh, R.; Mathers, R. T.; O'Reilly, R. K., Predicting Monomers for Use in Polymerization-Induced Self-Assembly. *Angew. Chem. Int. Ed.* **2018,** *57* (48), 15733-15737.

276. Le, D.; Dilger, M.; Pertici, V.; Diabaté, S.; Gigmes, D.; Weiss, C.; Delaittre, G., Ultra-Fast Synthesis of Multivalent Radical Nanoparticles by Ring-Opening Metathesis Polymerization-Induced Self-Assembly. *Angew. Chem. Int. Ed.* **2019,** *58* (14), 4725-4731.

277. Williford, J.-M.; Santos, J. L.; Shyam, R.; Mao, H.-Q., Shape control in engineering of polymeric nanoparticles for therapeutic delivery. *Biomat. Sci.* **2015,** *3* (7), 894-907; E. Hinde, K. Thammasiraphop, H. T. T. Duong, J. Yeow, B. Karagoz, C. Boyer, J. J. Gooding, K. Gaus, Pair correlation microscopy reveals the role of nanoparticle shape in intracellular transport and site of drug release. *Nat. Nanotechnol.* **2016**, (12), 81-89.

278. Geng, Y.; Dalhaimer, P.; Cai, S.; Tsai, R.; Tewari, M.; Minko, T.; Discher, D. E., Shape effects of filaments versus spherical particles in flow and drug delivery. *Nat. Nanotechnol.* **2007,** *2*, 249-255.

279. Champion, J. A.; Katare, Y. K.; Mitragotri, S., Making polymeric micro- and nanoparticles of complex shapes. *Proc. Natl. Aca. Sci.* **2007,** *104* (29), 11901; .

280. Kim, S.; Shi, Y.; Kim, J. Y.; Park, K.; Cheng, J.-X., Overcoming the barriers in micellar drug delivery: loading efficiency, in vivo stability, and micelle–cell interaction. *Expert Opinion on Drug Delivery* **2010,** *7* (1), 49-62.

281. Ye, Q.; Huo, M.; Zeng, M.; Liu, L.; Peng, L.; Wang, X.; Yuan, J., Photoinduced Reversible Worm-to-Vesicle Transformation of Azo-Containing Block Copolymer Assemblies Prepared by Polymerization-Induced Self-Assembly. *Macromolecules* **2018,** *51* (9), 3308-3314.

282. Schmelz, J.; Pirner, D.; Krekhova, M.; Ruhland, T. M.; Schmalz, H., Interfacial activity of patchy worm-like micelles. *Soft Matt.* **2013,** *9* (47), 11173-11177.

283. Schöbel, J.; Karg, M.; Rosenbach, D.; Krauss, G.; Greiner, A.; Schmalz, H., Patchy Wormlike Micelles with Tailored Functionality by Crystallization-Driven Self-Assembly: A Versatile Platform for Mesostructured Hybrid Materials. *Macromolecules* **2016,** *49* (7), 2761-2771.

284. Dai, X.; Zhang, Y.; Yu, L.; Li, X.; Zhang, L.; Tan, J., Seeded Photoinitiated Polymerization-Induced Self-Assembly: Cylindrical Micelles with Patchy Structures Prepared via the Chain Extension of a Third Block. *ACS Macro Lett.* **2019**, 955-961.

285. Bajorath, J., Integration of virtual and high-throughput screening. *Nat. Rev. Drug Discov.* **2002,** *1* (11), 882-894.

286. Wilms, D.; Klos, J.; Frey, H., Microstructured Reactors for Polymer Synthesis: A Renaissance of Continuous Flow Processes for Tailor-Made Macromolecules? *Macromol. Chem. Phys.* **2008,** *209* (4), 343-356.

287. Hoogenboom, R.; Fijten, M. W. M.; Abeln, C. H.; Schubert, U. S., High-Throughput Investigation of Polymerization Kinetics by Online Monitoring of GPC and GC. *Macromol. Rapid Commun.* **2004,** *25* (1), 237-242.

Graphical Abstract